greatly reduced the frequency of hypersensitivity reactions, an important dose-limiting toxic effect of oxaliplatin. A reduced incidence of hypersensitivity reactions to oxaliplatin enhances the effectiveness of mFOLFOX6 by allowing treatment to be prolonged. Our results were statistically significant, although the study was performed in a single institution. We therefore recommend our modified premedication regimen to reduce hypersensitivity reactions in clinical practice. Phase III prospective studies are highly warranted to confirm the effectiveness of modified premedication.

Conflict of interest No author has any conflict of interest.

References

1. Andre T, Boni C, Mounedji-Boudiaf L et al (2004) Oxaliplatin, fluorouracil, and leucovorin as adjuvant treatment for colon cancer. N Engl J Med 350:2343–2351
2. Rosique-Robles D, Vicent Verge JM, Borras-Blasco J et al (2007) Successful desensitization protocol for hypersensitivity reactions caused by oxaliplatin. Int J Clin Pharmacol Ther 45:606–610
3. Mis L, Fernando NH, Hurwitz HI et al (2005) Successful desensitization to oxaliplatin. Ann Pharmacother 39:966–969
4. Newman Taylor AJ, Cullinan P, Lympany PA et al (1999) Interaction of HLA phenotype and exposure intensity in sensitization to complex platinum salts. Am J Respir Crit Care Med 160:435–438
5. Zanotti KM, Rybicki LA, Kennedy AW et al (2001) Carboplatin skin testing: a skin-testing protocol for predicting hypersensitivity to carboplatin chemotherapy. J Clin Oncol 19:3126–3129
6. Kim BH, Bradley T, Tai J et al (2009) Hypersensitivity to oxaliplatin: an investigation of incidence and risk factors, and literature review. Oncology 76:231–238
7. Brandi G, Pantaleo MA, Galli C et al (2003) Hypersensitivity reactions related to oxaliplatin (OHP). Br J Cancer 89:477–481
8. Lenz G, Hacker UT, Kern W et al (2003) Adverse reactions to oxaliplatin: a retrospective study of 25 patients treated in one institution. Anticancer Drugs 14:731–733
9. Gowda A, Goel R, Berdzik J, et al (2004) Hypersensitivity reactions to oxaliplatin: incidence and management. Oncology (Williston Park) 18:1671–1675 (discussion 1676, 1680, 1683–1684)
10. Siu SW, Chan RT, Au GK (2006) Hypersensitivity reactions to oxaliplatin: experience in a single institute. Ann Oncol 17:259–261
11. Markman M, Kennedy A, Webster K et al (1999) An effective and more convenient drug regimen for prophylaxis against paclitaxel-associated hypersensitivity reactions. J Cancer Res Clin Oncol 125:427–429
12. Wrzesinski SH, McGurk ML, Donovan CT et al (2007) Successful desensitization to oxaliplatin with incorporation of calcium gluconate and magnesium sulfate. Anticancer Drugs 18:721–724
13. Pagani M, Bonadonna P, Senna GE et al (2008) Standardization of skin tests for diagnosis and prevention of hypersensitivity reactions to oxaliplatin. Int Arch Allergy Immunol 145:54–57
14. Giantonio BJ, Catalano PJ, Meropol NJ et al (2007) Bevacizumab in combination with oxaliplatin, fluorouracil, and leucovorin (FOLFOX4) for previously treated metastatic colorectal cancer: results from the Eastern Cooperative Oncology Group Study E3200. J Clin Oncol 25:1539–1544
15. Saltz LB, Clarke S, Diaz-Rubio E et al (2008) Bevacizumab in combination with oxaliplatin-based chemotherapy as first-line therapy in metastatic colorectal cancer: a randomized phase III study. J Clin Oncol 26:2013–2019
16. Goldberg RM, Sargent DJ, Morton RF et al (2006) Randomized controlled trial of reduced-dose bolus fluorouracil plus leucovorin and irinotecan or infused fluorouracil plus leucovorin and oxaliplatin in patients with previously untreated metastatic colorectal cancer: a North American Intergroup Trial. J Clin Oncol 24:3347–3353
17. Tournigand C, Andre T, Achille E et al (2004) FOLFIRI followed by FOLFOX6 or the reverse sequence in advanced colorectal cancer: a randomized GERCOR study. J Clin Oncol 22:229–237
18. Kitada N, Dan T, Takara K et al (2007) Oxaliplatin-induced hypersensitivity reaction displaying marked elevation of immunoglobulin E. J Oncol Pharm Pract 13:233–235
19. Maindrault-Goebel F, Andre T, Tournigand C et al (2005) Allergic-type reactions to oxaliplatin: retrospective analysis of 42 patients. Eur J Cancer 41:2262–2267

Biochemical and Biophysical Research Communications xxx (2011) xxx–xxx

Contents lists available at ScienceDirect

Biochemical and Biophysical Research Communications

journal homepage: www.elsevier.com/locate/ybbrc

Switching addictions between HER2 and FGFR2 in HER2-positive breast tumor cells: FGFR2 as a potential target for salvage after lapatinib failure

Koichi Azuma [a], Junji Tsurutani [a,*], Kazuko Sakai [b], Hiroyasu Kaneda [b], Yasuhito Fujisaka [a], Masayuki Takeda [a], Masahiro Watatani [c], Tokuzo Arao [b], Taroh Satoh [a], Isamu Okamoto [a], Takayasu Kurata [a], Kazuto Nishio [b], Kazuhiko Nakagawa [a]

[a] Department of Medical Oncology, Kinki University Faculty of Medicine, 377-2 Ohnohigashi, Osakasayama, Osaka 589-8511, Japan
[b] Department of Genome Biology, Kinki University Faculty of Medicine, 377-2 Ohnohigashi, Osakasayama, Osaka 589-8511, Japan
[c] Department of Surgery, Kinki University Faculty of Medicine, 377-2 Ohnohigashi, Osakasayama, Osaka 589-8511, Japan

ARTICLE INFO

Article history:
Received 27 February 2011
Available online xxxx

Keywords:
FGFR2
HER2
Lapatinib
Drug resistance
Breast cancer

ABSTRACT

Agents that target HER2 have improved the prognosis of patients with *HER2*-amplified breast cancers. However, patients who initially respond to such targeted therapy eventually develop resistance to the treatment. We have established a line of lapatinib-resistant breast cancer cells (UACC812/LR) by chronic exposure of *HER2*-amplified and lapatinib-sensitive UACC812 cells to the drug. The mechanism by which UACC812/LR acquired resistance to lapatinib was explored using comprehensive gene hybridization. The *FGFR2* gene in UACC812/LR was highly amplified, accompanied by overexpression of FGFR2 and reduced expression of HER2, and a cell proliferation assay showed that the IC_{50} of PD173074, a small-molecule inhibitor of FGFR tyrosine kinase, was 10,000 times lower in UACC812/LR than in the parent cells. PD173074 decreased the phosphorylation of FGFR2 and substantially induced apoptosis in UACC812/LR, but not in the parent cells. FGFR2 appeared to be a pivotal molecule for the survival of UACC812/LR as they became independent of the HER2 pathway, suggesting that a switch of addiction from the HER2 to the FGFR2 pathway enabled cancer cells to become resistant to HER2-targeted therapy. The present study is the first to implicate FGFR in the development of resistance to lapatinib in cancer, and suggests that FGFR-targeted therapy might become a promising salvage strategy after lapatinib failure in patients with HER2-positive breast cancer.

1. Introduction

Breast cancer is the second most frequent malignancy worldwide, and the prognosis of patients with metastatic disease still remains very poor, despite intensive research and drug development [1]. Amplification of the human epidermal growth factor receptor 2 (HER2) gene has been detected in 20–30% of human breast cancers, driving tumor development and being associated with a poor outcome [2]. HER2 forms dimers to become active, and its dimerization partners are the epidermal growth factor receptor (EGFR), HER2 itself, and HER3 in most cases. Since EGFR is a molecule frequently expressed in HER2-positive breast cancer, interaction between EGFR and HER2 could be important for the maintenance of oncogenesis [3]. Thus, targeting HER2 and EGFR together appears to be a promising therapeutic strategy for patients with *HER2*-amplified breast cancer, and multi-targeted small-molecule inhibitors such as lapatinib, BIBW2992 and AZD8931, directed against EGFR family members, have been developed for this purpose. Lapatinib binds to the ATP binding sites of EGFR and HER2, thus inhibiting their tyrosine kinase activity [4].

Acquired resistance to HER2-targeted drugs is one of the major obstacles to further improvement of clinical outcomes in this field, and research efforts have been focused on clarifying the mechanisms by which cancer cells acquire resistance to lapatinib. Several mechanisms of resistance to trastuzumab, a humanized monoclonal antibody against HER2, have been proposed, such as the presence of a truncated form of HER2 without an extracellular domain, loss of PTEN, and *PIK3CA* mutations in pre-clinical models, and such mechanisms may also have some implications for the lapatinib resistance phenotype [5–7]. In addition, overexpression of AXL, a receptor type kinase, has been reported to be a critical player for bypassing lapatinib-elicited HER2-PI3K-Akt signaling and conferring resistance to the drug in a breast cancer cell line [8].

Abbreviations: FGFR2, fibroblast growth factor receptor 2; HER2, human epidermal growth factor receptor 2; TKI, tyrosine kinase inhibitor; EGFR, epidermal growth factor receptor; IC_{50}, median inhibitory concentration; siRNA, small interfering RNA; Erk, extracellular signal-regulated kinase; RNAi, RNA interference; CGH, comprehensive gene hybridization.

* Corresponding author.
E-mail address: tsurutani_j@dotd.med.kindai.ac.jp (J. Tsurutani).

0006-291X/$ - see front matter © 2011 Elsevier Inc. All rights reserved.
doi:10.1016/j.bbrc.2011.03.002

Please cite this article in press as: K. Azuma et al., Switching addictions between HER2 and FGFR2 in HER2-positive breast tumor cells: FGFR2 as a potential target for salvage after lapatinib failure, Biochem. Biophys. Res. Commun. (2011), doi:10.1016/j.bbrc.2011.03.002

Fibroblast growth factor receptor 2 (FGFR2) is a member of the FGFR tyrosine kinase family, and consists of 4 receptors and 23 ligands [9]. Ligand binding leads to FGFR2 dimerization, autophosphorylation, and activation of signaling components including Akt and Erk kinases. Amplification and overexpression of the *FGFR2* gene is observed in gastric cancer and breast cancer [9], and single-nucleotide polymorphisms (SNPs) of the *FGFR2* gene are associated with a higher risk of sporadic breast cancer [10]. These features suggest that *FGFR2* may have an oncogene-like character, and be capable of transforming normal cells. This gene could act as a driving force for transformation of cancer cells into a further malignant phenotype, and constitute a potential target of treatment in cancer patients whose tumors express the protein.

Here we report that subpopulations of cells with *FGFR* gene amplification play a pivotal role in development of resistance to lapatinib in HER2-positive breast cancer.

2. Materials and methods

2.1. Cell culture and reagents

A human breast cancer cell line, UACC812 was obtained from the American Type Culture Collection (Manassas, VA), and cultured under a humidified atmosphere of 5% CO_2 at 37 °C in RPMI 1640 medium (Sigma, St. Louis, MO) supplemented with 10% fetal bovine serum. Gefitinib was obtained from Kemprotec Ltd. (UK). Lapatinib was obtained from Chemietek (Indianapolis, IN). PD173074 was purchased from Sigma (St. Louis, MO).

2.2. Generation of a lapatinib-resistant line and floating line from UACC812

The UACC812 cells were grown initially in medium containing 0.01 μM lapatinib, and the concentration was gradually increased up to 1 μM over the following 8 months to establish lapatinib-resistant cell lines (UACC812/LR).

2.3. Array-based comparative genomic hybridization

The Genome-wide Human SNP Array 6.0 (Affymetrix, Santa Clara, CA) was used to perform array-CGH on genomic DNA from each of the cell lines, in accordance with the manufacturer's instructions. A total of 250 ng of genomic DNA was digested with the restriction enzymes Nsp I and Sty I in independent parallel reactions (SNP6.0), ligated to the adaptor, and amplified using PCR with a universal primer and TITANIUM Taq DNA Polymerase (Clontech). The PCR products were quantified, fragmented, end-labeled, and hybridized onto a Genome-wide Human SNP Array 6.0. After washing and staining in Fluidics Station 450 (Affymetrix), the arrays were scanned to generate CEL files using the GeneArray Scanner 3000 and GeneChip Operating Software ver.1.4. In the array-CGH analysis, sample-specific changes in copy number were analyzed using Partek Genomic Suite 6.4 software (Partek Inc., St. Louis, MO).

2.4. Growth assay in vitro

Cells were cultured in 96-well flat-bottomed plates for 24 h before exposure to various concentrations of drugs for 72 h. TetraColor One (5 mM tetrazolium monosodium salt and 0.2 mM 1-methoxy-5-methyl phenazinium methylsulfate; Seikagaku, Tokyo, Japan) was then added to each well, and the cells were incubated for 3 h at 37 °C before measurement of absorbance at 490 nm with a Multiskan Spectrum instrument (Thermo Labsystems, Boston, MA). Absorbance values were expressed as a percentage relative to untreated cells, and the concentration of tested drugs resulting in 50% growth inhibition (IC_{50}) was calculated using the Prism program (GraphPad, San Diego, CA).

2.5. Cell death assay

After incubation, cells were harvested by trypsinization and resuspended in a solution of 1 μg/mL propidium iodide in PBS, then immediately acquired on the FL3 channel of a flow cytometer. The population of propidium iodide-positive cells was considered dead, whereas the propidium iodide-negative population was considered viable.

2.6. Immunoblot analysis

Cells were washed twice with ice-cold PBS and then lysed with 1× Cell Lysis Buffer (Cell Signaling Technology) containing 20 mM Tris–HCl (pH 7.5), 150 mM NaCl, 1 mM EDTA, 1% Triton X-100, 2.5 mM sodium pyrophosphate, 1 mM phenylmethylsulfonyl fluoride, and leupeptin (1 μg/ml). The protein concentration of cell lysates was determined with a BCA protein assay kit (Thermo Fisher Scientific), and equal amounts of protein were subjected to SDS–PAGE on a 4–12% gradient gel. The separated proteins were transferred to a PVDF membrane, which was then incubated with Blocking One solution (Nakarai Tesque, Kyoto, Japan) for 20 min at room temperature before incubation overnight at 4 °C with primary antibodies, including those against phosphorylated FGFR, phosphorylated EGFR(Y1086), phosphorylated HER2(Y1221/1222), EGFR, FGFR1, FGFR3, FGFR4, phosphorylated AKT, AKT, ERK, PARP, caspase-3 (Cell Signaling Technology, Danvers, MA), HER2 (Millipore), FGFR2 (Bek) and phosphorylated ERK (Santa Cruz Biotechnology) or β-actin (1:5000 dilution, Sigma). The membrane was then washed with PBS containing 0.05% Tween 20 before incubation for 1 h at room temperature with horseradish peroxidase-conjugated antibody against rabbit immunoglobulin G (Sigma). Immune complexes were finally detected using ECL Western blotting detection reagents (GE Healthcare, Little Chalfont, UK). The RTK array was purchased from R & D Systems (Minneapolis, MN) and used in accordance with the manufacturer's instructions.

2.7. Assay of phospho-FGFR2 activity

The activity of p-FGFR2 in cell lysates was measured using ELISA in accordance with the manufacturer's procedures (Human phosphor-FGFR2 Duoset; R & D Systems). The lysates were prepared as described above. All samples were run in triplicate assays. Color intensity was measured at 450 nm using a spectrophotometric plate reader. Growth factor concentrations were determined by comparison with standard curves.

2.8. FGFR2 gene silencing using small interfering RNA

Cells were plated at 50–60% confluence in six-well plates or 25 cm^2 flasks and then incubated for 24 h before transient transfection for 48 h with small interfering RNAs (siRNAs) mixed with Lipofectamine reagent (Invitrogen, Carlsbad, CA). A siRNA specific for FGFR2 mRNA and a nonspecific siRNA (control) were obtained from Nippon EGT (Toyama, Japan). The cells were then subjected to flow cytometry and immunoblot analysis.

2.9. Immunohistochemistry (IHC)

Paraffin-embedded tissue samples were cut at a thickness of 4 μM and examined on coated glass slides, after labeling with antibodies directed against the following using the ChemMate ENVISION method (DakoCytomation, Glostrup, Denmark). Endogenous

Please cite this article in press as: K. Azuma et al., Switching addictions between HER2 and FGFR2 in HER2-positive breast tumor cells: FGFR2 as a potential target for salvage after lapatinib failure, Biochem. Biophys. Res. Commun. (2011), doi:10.1016/j.bbrc.2011.03.002

peroxidase activity was inhibited by incubating the slides in 3% H_2O_2 for 20 min. FGFR2 (C-17, Santa Cruz Biotechnology) antigen retrieval was done by microwaving for 10 min in Target Citrate Solution (pH 6.0). Each slide was incubated overnight with the antibody at 4 °C. For staining detection, the ChemMate ENVISION method was used with DAB as the chromogen. The expression of FGFR2 protein in the cell membrane and cytoplasm was investigated in detail. FGFR2 expression was classified into three categories: score 0, no staining at all; or membrane expression in <10% of cancer cells; score 1+, faint/barely perceptible partial membrane expression in ⩾10% of cancer cells; score 2+, weak to moderate expression on the entire membrane in ⩾10% of the cancer cells; score 3+, strong expression on the entire membrane in ⩾10% of cancer cells. All IHC studies were evaluated by two IHC-experienced reviewers (K.A. and J.T.) who were blind to the conditions of the patients. Consistent results were obtained in 14 out of 16 samples, and two IHC samples without consistency were subjected to scoring by a third reviewer who was also blinded to the clinical information and scores assigned previously by the other two reviewers. Then, the majority scores were employed as the final results.

2.10. Study population and survival analysis

All patients received lapatinib between 2009 and 2010 at Kinki University School of Medicine. Sixteen tumors from a series of 13 patients diagnosed as having HER2-positive metastatic breast cancer were collected from the files of the Pathology Department, Kinki University School of Medicine, covering the period between 2009 and 2010. The HER2 status was considered positive if the local institution reported grade 3+ staining intensity (on a scale of 0–3) by means of IHC analysis or grade 2+ staining intensity by means of IHC analysis with gene amplification on fluorescence in situ hybridization. Details of the patients' clinical characteristics, including age, hormone status, prior therapy, and tumor response were obtained from chart review by an independent reviewer who was unaware of the results of IHC analysis. Tumor responses were evaluated after chemotherapy according to the Response Evaluation Criteria for Solid Tumors (RECIST). Four sites of metastasis were included. Any material that had been poorly fixed and/or had low cellularity was rejected. Paraffin-embedded tissues were obtained, and histologic examination of slides stained with hematoxylin-eosin and saffron was carried out by a specialist. All patients provided written informed consent for collection of their tissue material and clinical data for research purposes, and the tissue procurement protocol was approved by the institutional review board.

Progression-free survival was defined as the time between the onset of chemotherapy and the date when disease progression began. Patients without progression were regarded as censored at the date of the last follow-up. Curves for progression-free survival were estimated by the Kaplan–Meier method, and differences in survival functions were compared by the log-rank test.

All tests were two-sided, and differences at $P < 0.05$ were considered statistically significant. All the statistical analyses were conducted using JMP version 8 software (SAS Institute Inc., Cary, NC).

2.11. Fluorescence in situ hybridization

The gene copy number per cell for *HER2* was determined by fluorescence in situ hybridization (FISH) with the use of *HER2/neu* (17q11.2–q12) Spectrum Orange and CEP17 (chromosome 17 centromere) Spectrum Green probes (Vysis; Abbott, Des Plaines, IL). Gene amplification was defined as a mean *HER2*/chromosome 17 copy number ratio of >2.

2.12. Statistics

Experimental values were expressed ±SE. Statistical comparison of mean values was done using Student's *t* test.

3. Results

3.1. Establishment of lapatinib-resistant breast cancer cells

The UACC812 cells were grown initially in medium containing 0.01 μM lapatinib, and the concentration was gradually increased to 1 μM over the following 8 months to establish lapatinib-resistant cell lines (UACC812/LR). Cell growth assays were performed for the UACC812 cells and the UACC812/LR cells with various doses of lapatinib and gefitinib, as indicated in Fig. 1A, and the IC_{50} values were determined (Fig. 1A inset). UACC812/LR cells were resistant to lapatinib and gefinitib in comparison with the parent cells, the IC_{50} values for lapatinib (4.2433 ± 0.5066 μM) and gefitinib (11.1300 ± 0.5474 μM) being 42 times and 6 times higher than those in UACC812 (0.1006 ± 0.0053 μM and 1.9223 ± 0.3744 μM), respectively, but no differences were seen between the two cell lines in terms of the IC_{50} values for cisplatin and 5-FU (Fig. 1A inset), suggesting that chronic exposure of the UACC812 cells to lapatinib had induced resistance specific to EGFR or HER2 inhibitors.

3.2. FGFR2 gene amplification in UACC812/LR

To overview the chromosomal divergences between the parent cell line and its derivative, comprehensive gene hybridization (CGH) analyses were performed as described in Section 2. This revealed that the UACC812/LR cells harbored an amplification of the fibroblast growth factor receptor 2 (FGFR2) gene, the gene copy number in UACC812/LR being approximately 20 times that in UACC812 (Fig. 1B). Lysates of the parent and the derivative cells were subjected to Western blotting-based high-throughput analysis for expression of various receptor type kinases (RTK), and a dramatic increase in the expression of FGFR2 was observed in UACC812/LR relative to UACC812 (Fig. 1C). In contrast, the expression of HER2 was reduced in UACC812/LR in comparison to the parent cells (Fig. 1C upper panel). HER2-FISH analysis revealed that the *HER2* gene amplification was present in UACC812 cells, but not in UACC812/LR cells (Fig. 1C lower panel). To examine the role of FGFR2 in the growth of the parent cells and their derivative, an FGFR-TKI, PD173074, was utilized, and cell growth assays were performed for UACC812 and UACC812/LR treated with various concentrations of PD173074. UACC812/LR was more sensitive than UACC812 to PD173074, the IC_{50} (0.00121 ± 0.0034 μM) being 10,000 times lower than that for the parent cells (10.3373 ± 1.6629 μM), indicating that UACC812/LR cells had acquired dependency on the FGFR2 pathway, whereas FGFR2 played no role in the cell growth of UACC812 (Fig. 1D and inset).

3.3. UACC812/LR shows high phosphorylation of FGFG2 and undergoes apoptosis upon exposure to a FGFR tyrosine kinase inhibitor

To further evaluate the findings of the RTK arrays and cell growth assays, Western blotting was performed for biochemical profiling of these cell lines. Overexpression of phosphorylated FGFR2 (p-FGFR2) and native FGFR2, and downregulation of p-HER2 and p-EGFR in UACC812/LR cells relative to the parent cells were observed (Fig. 2A). The two cell lines were treated with lapatinib (1 μM) or PD173074 (0.1 and 1 μM) for 24 h, and the cell lysates were then subjected to Western blot analysis. The basal levels of p-EGFR, p-HER2 and native HER expression were

Please cite this article in press as: K. Azuma et al., Switching addictions between HER2 and FGFR2 in HER2-positive breast tumor cells: FGFR2 as a potential target for salvage after lapatinib failure, Biochem. Biophys. Res. Commun. (2011), doi:10.1016/j.bbrc.2011.03.002

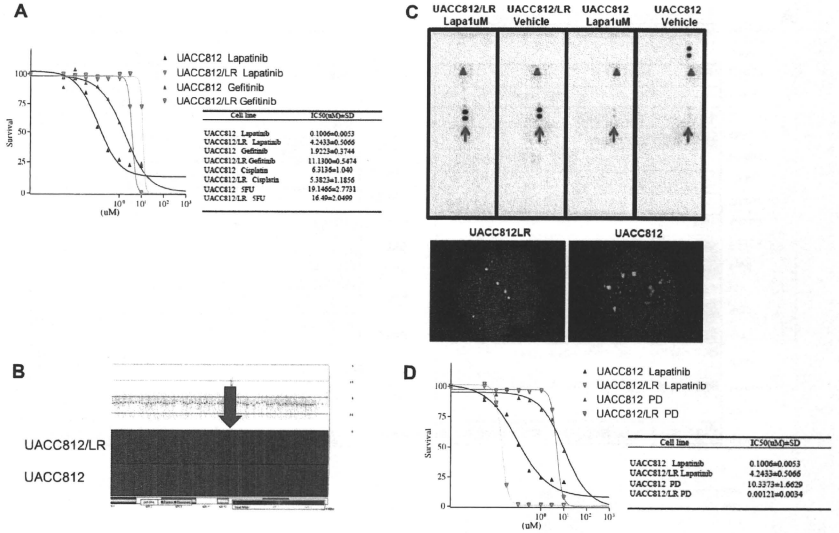

Fig. 1. Lapatinib-resistant cancer cells harbor *FGFR2* gene amplification, and are preferentially sensitive to an FGFR-TKI. (A) Cell growth assays were performed using UACC812 cells and their derivative, UACC812/LR cells, treated with lapatinib, gefitinib, cisplatin or 5-FU for 72 h, and IC_{50} values are shown in the inset. Results represent the mean ± SE of three experiments performed in triplicate. (B) *FGFR2* gene amplification detected in UACC812/LR cells. Comprehensive gene hybridization analysis revealed that the gene on chromosome 10q26 was highly amplified in UACC812/LR relative to its parent cell line. (C) Lysates from UACC812 cells and UACC812/LR cells treated with vehicle or 1 μM lapatinib for 6 h were subjected to Western blotting-based high-throughput analysis for RTKs. Arrows and arrowheads indicate signals for FGFR2 and HER2, respectively. Left column: UACC812/LR cells treated with 1 μM lapatinib; Second column from left: UACC812/LR treated with vehicle; Second column from right: UACC812 cells treated with 1 μM lapatinib; Right column: UACC812 cells treated with vehicle. Images of HER2-FISH analyses in UACC812 and UACC812/LR are shown. (D) Cell growth assays were performed using UACC812 cells and UACC812/LR cells with lapatinib or PD173074 at various doses for 72 h. IC_{50} values are shown in the inset. Results represent the mean ± SE of three experiments performed in triplicate.

decreased, and those of p-FGFR and native FGFR2 were dramatically increased in UACC812/LR cells (Fig. 2A). Lapatinib inhibited the expression of p-HER2 and p-EGFR accompanied by downregulation of p-Akt and p-Erk in UACC812 cells, but no inhibition of the phosphorylation of these signal components was observed in UACC812/LR (Fig. 2A). On the other hand, PD173074 did not affect the level of phosphorylated Akt or Erk in the parent cells, but inhibited that of p-FGFR along with p-Akt and p-Erk in UACC812/LR cells (Fig. 2A). Cleaved poly (ADP-ribose) polymerase (PARP) and caspase 3 as markers of apoptosis were increased in UACC812 and UACC812/LR after treatment with lapanib or PD173074, respectively, suggesting that the parent cells and their derivative were dependent on the different pathways for survival (Fig. 2A). Since a pan-antibody against p-FGFR was utilized in the Westen blotting to detect the pharmacological activity of PD173074, we further examined p-FGFR2 in an ELISA assay using a specific antibody against p-FGFR2 in UACC812 and UACC812/LR cells treated with lapatinib or PD173074 (Fig. 2B). We found that the basal level of p-FGFR2 was increased in UACC812/LR relative to the parent cells, and that phosphorylation was inhibited by PD173074 but not by lapatinib. Induction of cell death with lapatinib and/or pharmacological or genetic abrogation of FGFR2 was then measured in UACC812 and UACC812/LR cells (Fig. 2D). Cell death was induced in UACC812 cells treated with lapatinib but not in those treated with PD173074 (Fig. 2D left panel) or si-RNA for FGFR2 (Fig. 2D right panel). There were no increases in the percentage of cell death induced by lapatinib upon addition of PD173074 or si-RNA for FGFR2 in UACC812 cells or UACC812/LR (Fig. 2D left panel and right panel). Nonetheless, PD173074 and si-RNA for FGFR2 dramatically induced cell death in UACC812/LR cells (Fig. 2D left panel and right panel). Validation of the biochemical effects of si-RNA treatment on FGFR2 is shown in Fig. 2C. Overexpression of FGFR2 was observed in UACC812/LR cells relative to UACC812 cells, and treatment with si-RNA for FGFR2 reduced the expression of FGFR2, accompanied by inhibition of p-Akt and p-Erk in UACC812/LR cells (Fig. 2C). Cleaved PARP and caspase 3 were induced in UACC812 cells and UACC812/LR cells treated with lapatinib and/or si-RNA for FGFR2, respectively (Fig. 2C). Together, these findings suggested that UACC812/LR cells had become addicted to the FGFR2 pathway for survival in the absence of the activated HER2 pathway during the development of resistance to lapatinib.

3.4. High expression of FGFR2 in tumor specimens is associated with poor response to lapatinib

To further evaluate the role of FGFR2 in a clinical setting, we examined tissue specimens obtained from 13 consecutive patients with metastatic HER2-positive breast cancer treated with lapatinib between 2009 and 2010 at our institution. The median age of the patients was 60 years (35–69 years) and the median follow-up time after administration of lapatinib was 275 days (42–358 days). All the patients had been treated with lapatinib, and the

Please cite this article in press as: K. Azuma et al., Switching addictions between HER2 and FGFR2 in HER2-positive breast tumor cells: FGFR2 as a potential target for salvage after lapatinib failure, Biochem. Biophys. Res. Commun. (2011), doi:10.1016/j.bbrc.2011.03.002

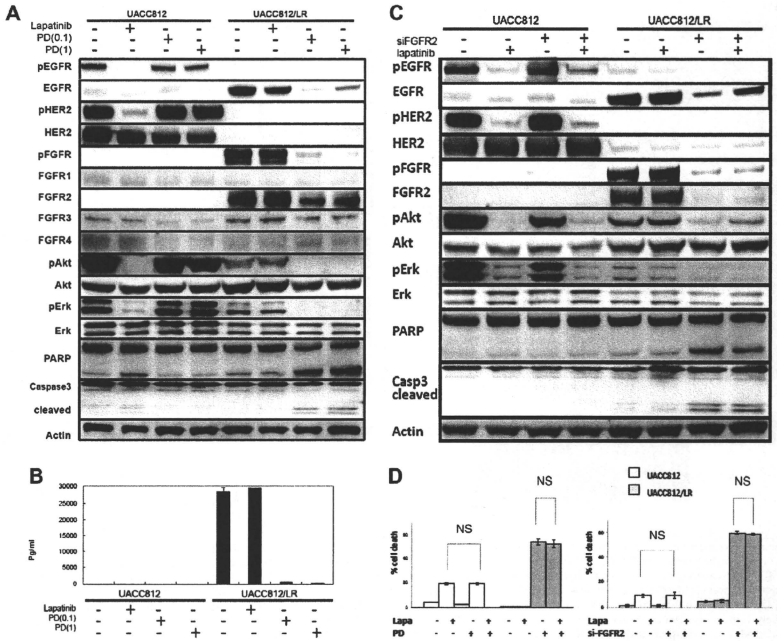

Fig. 2. FGFR2 is active in the lapatinib-resistant cell line, UACC812/LR, but not in the parental cells. (A) UACC812 cells and UACC812/LR cells were treated with 1 μM lapatinib, or 0.1 or 1 μM PD173074 for 24 h, as described in Section 2. Lysates were subjected to Western blotting with the indicated antibodies. (B) Phospho-FGFR2 levels were measured in UACC812 cells and UACC812/LR cells treated with vehicle, 1 μM lapatinib, or 0.1 or 1 μM PD173074 using an ELISA-based assay. Results represent the mean ± SE of three experiments performed in triplicate. (C) UACC812 cells and UACC812/LR cells were treated with 1 μM lapatinib and/or si-RNA for FGFR2 for 24 h after completion of transfection. Lysates were subjected to Western blotting with the indicated antibodies. (D) UACC812 cells and UACC812/LR cells were treated with 1 μM lapatinib and/or 0.1 μM PD173074 for 48 h (left panel) or with 1 μM lapatinib and/or si-RNA for FGFR2 for 48 h after completion of transfection (right panel). The cells were harvested and subjected to flow cytometry analysis to assess the extent of cell death. Results represent the mean ± SE of three experiments performed in triplicate. NS, not statistically significant.

Table 1
Clinicopathological features of HER2 positive MBC.

Patients #	Age	Primary hormone receptor status	Prior therapy	Response*	FGFR2 expression
1	52	ER+, PgR+	H, T, A	SD	0
2	53	ER+, PgR−	H, A	SD	1+
3	47	ER+, PgR−	H, T, A	PR	1+
4	60	ER+, PgR−	H, T	SD	1+
5	69	ER−, PgR−	H, T, A	PD	2+
6	67	ER−, PgR−	H	NE	1+
7	52	ER+, PgR−	H, T	PD	0
8	47	ER−, PgR−	H, T, A	SD	1+
9	35	ER+, PgR+	H , T, A	PR	1+
10	65	ER−, PgR−	H, T, A	NE	0
11	61	ER−, PgR−	H , T, A	PD	2+
12	69	ER+, PgR+	H, T, A	PD	2+
13	59	ER−, PgR−	H, T	PR	0

MBC, metastatic breast cancer; ER, estrogen receptor; PgR, progesterone receptor; CR, complete response; PR, partial response; SD, stable disease; PD, progressive disease; NE, not evaluable; H, Herceptin; T, Taxanes; A, Anthracycline.
* Response to lapatinib-containing regimens.

clinicopathological features including IHC scores of FGFR2 in tumor specimens are summarized in Table 1. Time to progression (TTP) while receiving the treatment was plotted using Kaplan–Meier curves stratified by FGFR2 expression (score 0, 1 vs. 2, 3, Fig. 3), and the patients with FGFR2-overexpressing tumors had significantly poor survival ($P = 0.0082$), suggesting that FGFR2 may play at least a partial role in the development of resistance to lapatinib, probably through selection of FGFR2-overexpressing tumor cells.

4. Discussion

Several models have been proposed to account for the clinical resistance to HER2-targeted therapies including *PIK3CA* gene mutation and *AXL gene amplification* [5–8]. Gene sequence analyses revealed that UACC812 and UACC812/LR did not harbor *PIK3CA* gene mutation (data not shown), and Western blotting showed that UACC812/LR cells do not express AXL (data not shown), indicating that these two molecules are not causative factors for acquired resistance to lapatinib in UACC812/LR. Instead, the

Please cite this article in press as: K. Azuma et al., Switching addictions between HER2 and FGFR2 in HER2-positive breast tumor cells: FGFR2 as a potential target for salvage after lapatinib failure, Biochem. Biophys. Res. Commun. (2011), doi:10.1016/j.bbrc.2011.03.002

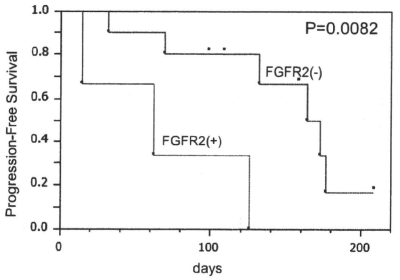

Fig. 3. Kaplan–Meier curves illustrating associations between protein expression and progression-free survival since the start of lapatinib. Survival curves are plotted as graphs according to FGFR2 expression level. The *P*-value was calculated using Log-rank test.

present model revealed amplification of *FGFR2* in lapatinib-resistant cells, and activation of FGFR2 substantially contributed to survival of the cells.

There is compelling evidence for deregulated FGF signaling in the pathogenesis of many cancers that originate from different tissue types. Aberrant FGF signaling can promote tumor development by directly driving cancer cell proliferation and survival. The underlying mechanism driving FGF signaling is largely tumor-specific, and can be attributed to genomic *FGFR* alterations that drive ligand-independent receptor signaling. Mutations of *FGFR2*, which are frequently extracellular, have been described in 12% of endometrial carcinomas [11]. *FGFR2*-mutant endometrial cancer cell lines are highly sensitive to FGFR tyrosine kinase inhibitors, suggesting oncogenic addiction of the cancer cells to the activated form of mutant FGFR [12]. In this study, gene sequencing analysis of *FGFR2* in UACC812 cells and UACC812/LR cells revealed no mutations, but gene amplification was noted in UACC812/LR in comparison with UACC812. Amplifications of *FGFR2* have been reported in approximately 10% of gastric cancers, and have been associated with poor prognosis [13]. Gastric cancer cell lines with *FGFR2* amplifications show ligand-independent signaling and are highly sensitive to FGFR inhibitors [13]. Inhibition of FGFR2 substantially induced cell death in UACC812 cells/LR harboring gene amplification of *FGFR2*, but not in UACC812 cells, and this was consistent with the above reports.

UACC812/LR cells showed loss of *HER2* amplification after chronic exposure to lapatinib, being reminiscent of clinical observations. Loss of *HER2* amplification following trastuzumab-based neoadjuvant systemic therapy has been reported in patients with residual breast cancers [14]. One third of patients with significant residual disease showed loss of *HER2* amplification, and this change was associated with poor relapse-free survival. We speculate that these residual tumors after trastuzumab-based therapy may have harbored alternative driving genes to support further tumor development under selection pressure with trastuzumab, and our model using UACC812/LR cells recapitulated the clinical loss of HER2 resulting from HER2-targeted therapies, although lapatinib was used instead of trastuzumab in this study.

Together, these findings suggest that FGFR2 may be a key molecule in the development of resistance to lapatinib in HER2-positive breast cancer through selection of cells with a growth advantage and improved survival, and that FGFR-targeted therapy may be a promising strategy for breast cancer patients in whom treatment with lapatinib has failed. Further clinical studies using a larger set of tumor specimens should be performed to confirm our findings in a small set of clinical samples, and development of FGFR-targeted therapy is warranted to clarify the role of FGFR in resistance to HER2-targeted medicines.

References

[1] J. Ferlay, H.R. Shin, F. Bray, et al., Estimates of worldwide burden of cancer in 2008, GLOBOCAN 2008, Int. Cancer. 127 (2010) 2893–2917.
[2] D.J. Slamon, G.M. Clark, S.G. Wong, et al., Human breast cancer: correlation of relapse and survival with amplification of the HER2/neu oncogene, Science 235 (1987) 177–182.
[3] M.P. DiGiovanna, D.F. Stern, S.M. Edgerton, et al., Relationship of epidermal growth factor receptor expression to ErbB-2 signaling activity and prognosis in breast cancer patients, J. Clin. Oncol. 20 (2005) 1152–1160.
[4] G.E. Konecny, M.D. Pegram, N. Venkatesan, et al., Activity of the dual kinase inhibitor lapatinib (GW572016) against HER-2-overexpressing and trastuzumab-treated breast cancer cells, Cancer Res. 66 (2006) 1630–1639.
[5] M. Scaltriti, F. Rojo, A. Ocana, et al., Expression of p95HER2, a truncated form of the HER2 receptor, and response to anti-HER2 therapies in breast cancer, J. Natl. Cancer Inst. 99 (2007) 628–638.
[6] D. Faratian, A. Goltsov, G. Lebedeva, et al., Systems biology reveals new strategies for personalizing cancer medicine and confirms the role of PTEN in resistance to trastuzumab, Cancer Res. 69 (2009) 6713–6720.
[7] P.J.A. Eichhorn, M. Gili, M. Scaltriti, et al., Phosphatidylinositol 3-kinase hyperactivation results in lapatinib resistance that is reversed by the mTOR/phosphatidylinositol 3-kinase inhibitor NVP-BEZ235, Cancer Res. 68 (2008) 9221–9230.
[8] L. Liu, J. Greger, H. Shi, et al., Novel mechanism of lapatinib resistance in HER2-positive breast tumor cells: activation of AXL, Cancer Res. 69 (2009) 6871–6878.
[9] N. Turner, R. Grose, Fibroblast growth factor signaling: from development to cancer, Nat. Rev. Cancer 10 (2010) 116–129.
[10] S.N. Stacey, A. Manolescu, P. Sulem, et al., Common variants on chromosome 5p12 confer susceptibility to estrogen receptor-positive breast cancer, Nat. Genet. 40 (2008) 703–706.
[11] A. Dutt, H.B. Salvesen, T.H. Chen, et al., Drug-sensitive FGFR2 mutations in endometrial carcinoma, Proc. Natl. Acad. Sci. USA 105 (2008) 8713–8717.
[12] D.M. Ornitz, P.J. Marie, FGF signaling pathways in endochondral and intramembranous bone development and human genetic disease, Genes Dev. 16 (2002) 1446–1465.
[13] K. Kunii, D.J. Gorenstein, H. Hatch, et al., FGFR2-amplified gastric cancer cell lines require FGFR2 and Erbb3 signaling for growth and survival, Cancer Res. 68 (2008) 2340–2348.
[14] E.A. Mittendorf, Y. Wu, M. Scaltriti, et al., Loss of HER2 amplification following trastuzumab-based neoadjuvant systemic therapy and survival outcomes, Clin. Cancer Res. 15 (2009) 7381–7388.

Please cite this article in press as: K. Azuma et al., Switching addictions between HER2 and FGFR2 in HER2-positive breast tumor cells: FGFR2 as a potential target for salvage after lapatinib failure, Biochem. Biophys. Res. Commun. (2011), doi:10.1016/j.bbrc.2011.03.002

Invest New Drugs
DOI 10.1007/s10637-010-9545-9

SHORT REPORT

Perirenal hematoma associated with bevacizumab treatment

Hidetoshi Hayashi · Isamu Okamoto · Kazuhiko Nakagawa

Received: 13 August 2010 / Accepted: 14 September 2010

Summary We now describe the first example of a patient who developed perirenal hematoma during the course of bevacizumab-containing chemotherapy. A 59-years-old woman with metastatic rectal cancer treated with bevacizumab, who developed low back pain after 11 cycles of chemotherapy. CT-scan was consistent with perirenal hematoma and discontinuation of bevacizumab resulted in symptomatic improvement. Nontraumatic perirenal hematoma is a rare condition that can cause shock in severe cases. Given that several types of bleeding complication are known to be associated with bevacizumab treatment, we concluded that bevacizumab likely contributed to the perirenal hematoma in this case. Although the appropriate modification of bevacizumab treatment in the setting of perirenal hematoma is still unclear, physicians should be aware of this potential bevacizumab-associated bleeding complication.

Keywords Bevacizumab · Perirenal hematoma · VEGF · Rectal cancer

A 59-year-old woman was diagnosed with rectal cancer accompanied by multiple liver metastases in March 2009. A palliative rectectomy was performed to resolve partial rectal obstruction, but thereafter the patient refused to receive systemic chemotherapy. Four months later, she presented with symptoms of tumor progression and abdominal pain. Computed tomography (CT) revealed progression of multiple hepatic metastases, and she was placed on salvage therapy of FOLFOX and bevacizumab (5 mg/kg, intravenous, for 90 min biweekly) after she gave her full informed consent. After the third cycle of treatment, a partial response was confirmed by CT and treatment was continued with no severe adverse effects. After 11 cycles of FOLFOX with bevacizumab, however, the patient complained of low back pain, which was not associated with microscopic hematuria. Positron emission tomography–CT revealed progression of disease with recurrence in peritoneal metastasis with hydronephrosis. In addition, a mass around the left kidney, which was round and sharply marginated with homogeneously high attenuation, was observed (Fig. 1, with the mass indicated by the arrow). Although the mass was not evaluated surgically, its appearance was suggestive of a nontraumatic perirenal hematoma, and an urologist recommended adoption of a wait-and-see approach. The patient was immediately instructed to discontinue chemotherapy including bevacizumab. CT examination 2 weeks later revealed the size of the perirenal mass to be stable. The low back pain of the patient was relieved with complete bed rest.

Vascular endothelial growth factor (VEGF) is a proangiogenic molecule that has been implicated in several steps of normal and pathologic angiogenic processes. Bevacizumab, a humanized monoclonal antibody specific for VEGF, shows substantial activity against various types of solid tumor. Bleeding complications, including epistaxis, hemoptysis, hematemesis, gastrointestinal or vaginal bleeding, and brain hemorrhage, have been observed in patients treated with the combination of chemotherapy and bevacizumab [1]. Patients with colorectal cancer who receive bevacizumab plus chemotherapy generally show a higher incidence of serious hemorrhage (3 to 9%) than do those on chemotherapy alone [2–5]. With regard to a possible explanation for the high incidence of bleeding following bevacizumab treatment [6],

H. Hayashi · I. Okamoto (✉) · K. Nakagawa
Department of Medical Oncology,
Kinki University Faculty of Medicine,
377-2 Ohno-higashi, Osaka-Sayama,
Osaka 589-8511, Japan
e-mail: chi-okamoto@dotd.med.kindai.ac.jp

Published online: 24 September 2010

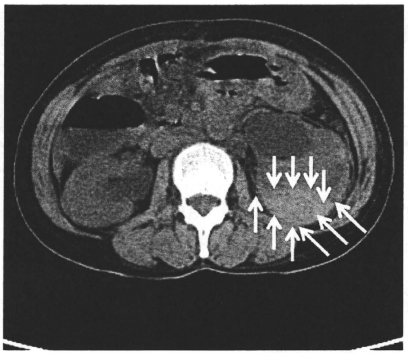

Fig. 1 A mass around the left kidney, which was round and sharply marginated with homogeneously high attenuation

VEGF not only stimulates endothelial cell proliferation during new tumor vessel formation but also promotes endothelial cell survival and helps maintain vascular integrity. Inhibition of VEGF signaling might therefore interfere with the regenerative capacity of endothelial cells and induce defects in the endothelial layer that expose the underlying matrix, leading to hemorrhage.

Nontraumatic perirenal hematoma is rare, whereas traumatic perirenal hematoma commonly results from renal injury or occurs as a severe complication after kidney-damaging surgery or other procedures. The most frequently identified cause of nontraumatic perirenal hematoma is renal neoplasms [7], with vascular disease, such as polyarteritis nodosa, being the second. In addition, antiplatelet therapy has been identified as an underlying cause of drug-induced perirenal hematoma [8]. Symptoms of perirenal hematoma include flank or abdominal pain, either gross or microscopic hematuria, and, in severe cases, signs of shock. CT is the valuable examination for diagnosis of perirenal hematoma [9].

The present patient complained of pain in the low back region and denied any relevant past history, including renal neoplasms, vascular disease, and antiplatelet therapy. CT findings were compatible with perirenal hematoma, which is visualized as fluid collection of high attenuation. To our knowledge, no reports associate FOLFOX with the development of perirenal hematoma or other type of hemorrhage with the exception of gastrointestinal bleeding caused by thrombocytopenia. Given that several types of bleeding complication are known to be associated with bevacizumab treatment, we concluded that bevacizumab likely contributed to the perirenal hematoma in this case.

Bevacizumab was discontinued and the patient was followed closely without surgical intervention. As a result, her symptoms resolved without a further increase in volume of the perirenal hematoma as evaluated by CT. To the best of our knowledge, this is the first reported case of the potential association of perirenal hematoma with bevacizumab therapy. Although the appropriate modification of bevacizumab treatment in the setting of perirenal hematoma is unclear, a conservative approach in this patient led to symptomatic improvement. Given the increasing number of patients receiving bevacizumab, physicians should be aware of this potential bevacizumab-associated complication.

Conflict of interest The authors declare no conflicts of interest.

References

1. Elice F, Rodeghiero F (2010) Bleeding complications of antiangiogenic therapy: pathogenetic mechanisms and clinical impact. Thromb Res 125(Suppl 2):S55–S57
2. Kabbinavar F, Hurwitz HI, Fehrenbacher L, Meropol NJ, Novotny WF, Lieberman G et al (2003) Phase II, randomized trial comparing bevacizumab plus fluorouracil (FU)/leucovorin (LV) with FU/LV alone in patients with metastatic colorectal cancer. J Clin Oncol 21:60–65
3. Hurwitz H, Fehrenbacher L, Novotny W, Cartwright T, Hainsworth J, Heim W et al (2004) Bevacizumab plus irinotecan, fluorouracil, and leucovorin for metastatic colorectal cancer. N Engl J Med 350:2335–2342
4. Kabbinavar FF, Schulz J, McCleod M, Patel T, Hamm JT, Hecht JR et al (2005) Addition of bevacizumab to bolus fluorouracil and leucovorin in first-line metastatic colorectal cancer: results of a randomized phase II trial. J Clin Oncol 23:3697–3705
5. Hurwitz H, Saini S (2006) Bevacizumab in the treatment of metastatic colorectal cancer: safety profile and management of adverse events. Semin Oncol 33(5 Suppl 10):S26–S34
6. Kilickap S, Abali Hs, Celik I (2003) Bevacizumab, bleeding, thrombosis, and warfarin. J Clin Oncol 21:3542, author reply 3
7. Zhang JQ, Fielding JR, Zou KH (2002) Etiology of spontaneous perirenal hemorrhage: a meta-analysis. J Uro 167:1593–1596
8. Yamamoto K, Yasunaga Y (2005) Antiplatelet therapy and spontaneous perirenal hematoma. Int J Urol 12:398–400
9. Belville JS, Morgentaler A, Loughlin KR, Tumeh SS (1989) Spontaneous perinephric and subcapsular renal hemorrhage: evaluation with CT, US, and angiography. Radiology 172:733–738

Lung Cancer xxx (2010) xxx–xxx

Contents lists available at ScienceDirect

Lung Cancer

journal homepage: www.elsevier.com/locate/lungcan

Thymidylate synthase and dihydropyrimidine dehydrogenase expression levels are associated with response to S-1 plus carboplatin in advanced non-small cell lung cancer

Masayuki Takeda[a], Isamu Okamoto[a,*], Naoko Hirabayashi[b], Mami Kitano[a], Kazuhiko Nakagawa[a]

[a] Department of Medical Oncology, Kinki University Faculty of Medicine, 377-2 Ohno-higashi, Osaka-Sayama, Osaka 589-8511, Japan
[b] Pathological and Genetic Testing Section, SRL Incorporated, 3-5-5 Midorigaoka, Hamura-shi, Tokyo 205-0003, Japan

ARTICLE INFO

Article history:
Received 9 July 2010
Received in revised form 8 September 2010
Accepted 28 October 2010

Keywords:
Thymidylate synthase
Dihydropyrimidine dehydrogenase
Immunohistochemistry
Non-small cell lung cancer
S-1
Predictive marker

ABSTRACT

S-1 is an oral fluoropyrimidine derivative that is active against non-small cell lung cancer (NSCLC). Development of S-1 combination chemotherapy for advanced NSCLC is under way. Given the importance of designing therapeutic strategies based on specific tumor biology, we have evaluated the relation between immunohistochemical expression levels of thymidylate synthase (TS), orotate phosphoribosyltransferase (OPRT), or dihydropyrimidine dehydrogenase (DPD) and the response to treatment with S-1 plus carboplatin in patients with advanced NSCLC. Chemotherapy-naïve patients with advanced (stage IIIB or IV) NSCLC, an Eastern Cooperative Oncology Group performance status of 0 or 1, adequate organ function, and archival tumor tissue were assigned to receive S-1–carboplatin ($n = 22$). The predictive or prognostic relevance of the molecular markers was also examined by their evaluation in patients treated with paclitaxel plus carboplatin ($n = 25$). Expression levels of TS, OPRT, or DPD in tumor specimens did not differ significantly between patients treated with S-1–carboplatin and those treated with paclitaxel–carboplatin. A low expression level of TS or of DPD was associated with a better response and longer survival in patients treated with S-1–carboplatin but not in those treated with paclitaxel–carboplatin. Tumor expression levels of TS and DPD are predictive of response to S-1–carboplatin chemotherapy in patients with advanced NSCLC.

1. Introduction

Lung cancer is the most common cause of cancer-related death worldwide, with non-small cell lung cancer (NSCLC) accounting for ~75% of all lung cancer cases [1]. Platinum-based chemotherapy regimens are the standard first-line treatment for individuals with advanced NSCLC, but the efficacy of such regimens has reached a plateau [2]. Both experimental and clinical studies have revealed that many molecules contribute to the various biological behaviors of malignant tumors including NSCLC. New strategies based on a better understanding of tumor biology are thus needed to maximize the efficacy of current treatments. Indeed, certain molecular markers, such as excision-repair cross-complementation type 1 (ERCC1), ribonucleotide reductase subunit M1 (RRM1), and breast cancer 1 (BRCA1), have been associated with the sensitivity of NSCLC tumors to cisplatin-based regimens, although there is currently insufficient evidence to recommend their routine clinical use [3–5].

5-Fluorouracil (5-FU), a pyrimidine analog that is metabolized by pyrimidine metabolic pathways, has been used worldwide for chemotherapy in individuals with various solid organ malignancies. Encouraging clinical results have recently led to the development of a new generation of oral fluoropyrimidines, commonly referred to as dihydropyrimidine dehydrogenase (DPD)–inhibitory fluoropyrimidines (DIFs). S-1 is one anticancer agent developed on the basis of the DIF concept and contains the 5-FU prodrug tegafur, potassium oxonate, and 5-chloro-2,4-dihydroxypyridine (CDHP), an inhibitor of DPD. S-1 is active against a wide range of solid tumors including NSCLC, and the development of S-1 combination chemotherapy for advanced NSCLC is under way [6–10]. Phase I or II studies have shown that combination therapy with S-1 and platinum compounds (cisplatin or carboplatin) is feasible and well tolerated in patients with advanced NSCLC, with efficacy results similar to those obtained with other platinum doublets [7–9].

Several enzymes participate in the metabolic pathways of 5-FU or folate, including thymidylate synthase (TS), a target enzyme of 5-FU; DPD, which catalyzes the degradation of 5-FU; and orotate phosphoribosyltransferase (OPRT). Previous studies have demonstrated a correlation between the expression levels of TS, DPD, and

* Corresponding author. Tel.: +81 72 366 0221; fax: +81 72 360 5000.
E-mail address: chi-okamoto@dotd.med.kindai.ac.jp (I. Okamoto).

0169-5002/$ – see front matter © 2010 Elsevier Ireland Ltd. All rights reserved.
doi:10.1016/j.lungcan.2010.10.022

OPRT in solid tumors and 5-FU sensitivity [11]. However, the clinical relevance of these enzymes has not been established for NSCLC patients treated with S-1 or S-1 combination chemotherapy. We have now investigated the predictive value of TS, DPD, or OPRT expression in individuals with NSCLC treated with S-1 plus carboplatin (CBDCA). These molecular markers were also examined by their evaluation in patients treated with paclitaxel plus carboplatin.

2. Patients and methods

2.1. Patient characteristics

The present retrospective study recruited consecutive patients with advanced NSCLC who received chemotherapy at Kinki University Hospital between June 2003 and October 2009. Patients met all of the following criteria: a histological diagnosis of NSCLC with at least one measurable lesion; a clinical stage of IIIB or IV; an Eastern Cooperative Oncology Group (ECOG) performance status of 0 or 1; an age of 75 years or younger; adequate hematologic, hepatic, and renal function; treatment with CBDCA at an area under the curve (AUC) of 6 on day 1 and paclitaxel (PTX) at 200 mg/m^2 on day 1 or with CBDCA at an AUC of 5 on day 1 and S-1 at 80 mg/m^2 on days 1–14 every 3 weeks as first-line chemotherapy; and sufficient tissue available in paraffin blocks for assessment by immunohistochemistry. Tumor response was examined by computed tomography and was evaluated according to the Response Evaluation Criteria in Solid Tumors (RECISTs). Many patients had already died before the initiation of immunohistochemical analysis, preventing us from obtaining informed consent. The institutional review board therefore approved our study protocol with the conditions that samples would be processed anonymously and analyzed for protein expression and that the study would be disclosed publicly, according to the Ethical Guidelines for Human Genome Research published by the Ministry of Education, Culture, Sports, Science, and Technology, the Ministry of Health, Labor, and Welfare, and the Ministry of Economy, Trade, and Industry of Japan. The present study also conforms to the provisions of the Declaration of Helsinki.

2.2. Immunohistochemistry and scoring of protein expression

Sections (thickness, 4 μm) were depleted of paraffin with xylene and then rehydrated, and endogenous peroxidase activity was quenched by incubation with 0.3% hydrogen peroxide in methanol. The antigen retrieval was carried out by microwaving in citrate buffer, pH 6.0 (TS, OPRT) or in 1 mM EDTA, pH 8.0 (DPD) for 10 min. After washing in phosphate buffered saline, the sections were then incubated with polyclonal antibodies (Taiho Pharmaceutical Co., Saitama, Japan) to either TS (dilution of 1:100), OPRT (dilution of 1:1000), or DPD (dilution of 1:1350) overnight at room temperature. Biotinylated goat anti-rabbit IgG was applied as a secondary antibody for 30 min, followed by streptavidin–biotinylated peroxidase complex for 30 min at room temperature. Peroxidase activity was visualized with diaminobenzidine tetrahydrochloride (DAB) solution (DAKO Co. Ltd., Santa Barbara, CA), and counter staining was performed with hematoxylin. The human colon cancer cell line DLD-1/FrUrd, human breast cancer cell line MDA-MB-435S, and human pancreatic cancer cell line MIAPaCa-2 were used as positive controls for the staining of TS, OPRT, and DPD, respectively. All of the immunostained sections were reviewed by two observers (N.H. and K.N.) without knowledge of the patients' characteristics. Sections with discrepant results were jointly re-evaluated until a consensus was reached. Cytoplasmic staining for TS, OPRT, and DPD was scored in a semiquantitative manner reflecting both the intensity of staining and the percentage of cells with staining at each intensity. Staining intensity was classified as 0 (no staining), +1 (weak staining), +2 (distinct staining), or +3 (strong staining). A value designated the HSCORE was obtained as $\Sigma(I \times PC)$, where I and PC represent staining intensity and the percentage of cells that stain at each intensity, respectively. The selection of clinically important cutoff scores for TS, OPRT, or DPD expression was based on receiver operating characteristic (ROC) curve analysis.

Table 1
Patient characteristics.

Characteristic	S-1 plus CBDCA*n* (%)	PTX plus CBDCA*n* (%)
Sex		
Male	15 (68)	17 (68)
Female	7 (32)	8 (32)
Age (years)[a]	63 (39–73)	65 (48–74)
Smoking history		
Never-smoker	3 (14)	7 (28)
Smoker	19 (86)	18 (72)
Tumor histology		
Adenocarcinoma	16 (73)	16 (64)
Squamous cell	1 (4)	5 (20)
Other	5 (23)	4 (16)
Disease stage		
IIIB	3 (14)	4 (16)
IV	19 (86)	21 (84)
Tumor response[b]		
ORR (CR + PR)	9 (41)	9 (36)
SD	6 (27)	10 (40)
PD	7 (32)	6 (24)

[a] Data are presented as median (range).
[b] ORR, overall response rate; CR, complete response; PR, partial response; SD, stable disease; PD, progressive disease.

2.3. Statistical analysis

Expression levels of TS, OPRT, and DPD were compared between groups with the Mann–Whitney U test, and the relations between these variables were evaluated with Pearson's correlation test. Differences between the two treatment groups for demographic characteristics and the relation between treatment response and the expression of TS or DPD were evaluated with the two-sided Fisher's exact test. Overall survival and progression free survival were assessed from the first day of chemotherapy administration to the data of death from any cause and the date of objective disease progression, respectively. Patients without documented death at the time of the final analysis were evaluated at the date they were last known to be alive or of their last objective tumor assessment. The Kaplan–Meier method was used to estimate the probability of survival as a function of time, and differences in the survival of subgroups of patients were evaluated with the log-rank test. All P values were based on a two-tailed statistical analysis, and a P value of <0.05 was considered statistically significant. All statistical analysis was performed with GraphPad prism software (version 5.0; GraphPad Software, San Diego, CA).

3. Results

3.1. Patient characteristics

A total of 47 patients met the eligibility criteria (Table 1). Twenty-two patients were treated with S-1 plus CBDCA (S-1 arm) and 25 patients were treated with PTX plus CBDCA (PTX arm). Most (68%) patients were male in both groups. The median age of the patients was 63 years (range, 39–73) in the S-1 arm and 65 years (range, 48–74) in the PTX arm. Adenocarcinoma was the predominant histological type of NSCLC, accounting for 73% of patients

Please cite this article in press as: Takeda M, et al. Thymidylate synthase and dihydropyrimidine dehydrogenase expression levels are associated with response to S-1 plus carboplatin in advanced non-small cell lung cancer. Lung Cancer (2010), doi:10.1016/j.lungcan.2010.10.022

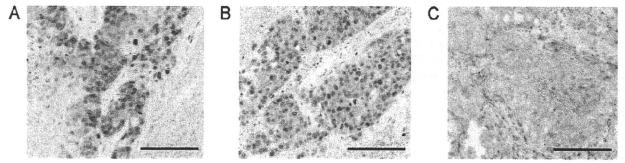

Fig. 1. Immunohistochemical staining of human NSCLC tissue. Representative sections of carcinomas with high levels of expression of TS (A), OPRT (B), or DPD (C) are shown. Scale bars, 125 μm.

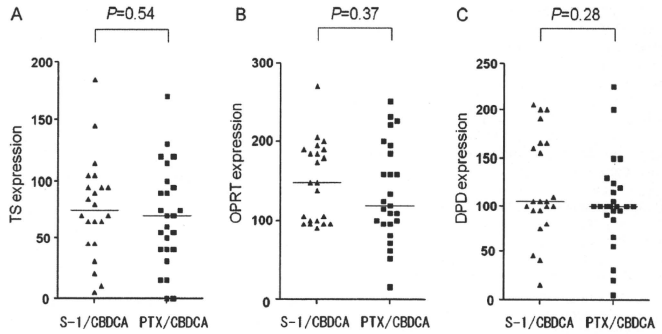

Fig. 2. Expression levels of TS (A), OPRT (B), and DPD (C) in NSCLC specimens of patients treated with S-1 plus CBDCA or with PTX plus CBDCA. Median values for expression level (HSCORE) are indicated by the horizontal lines. *P* values were determined with the Mann–Whitney *U* test.

in the S-1 arm and 64% in the PTX arm. The S-1 and PTX arms included 19 (86%) and 21 (84%) patients, respectively, with stage IV disease. There were no significant differences in sex distribution, age, smoking history, tumor histology, or disease stage between the S-1 and PTX arms. The median number of treatment cycles was 4 (range, 1–6) and 3 (range, 1–6) in the S-1 and PTX arms, respectively. The overall response rate (ORR = complete response [CR] + partial response [PR]) was 41% in the S-1 arm and 36% in the PTX arm (Table 1). The median follow-up time was 14.2 months, and the median overall survival was 15.5 months in the S-1 arm and 13.3 months in the PTX arm, with no significant difference in this parameter between the two arms ($P = 0.52$, log-rank test; data not shown).

3.2. Expression levels of TS, OPRT, and DPD in tumor specimens

We examined the expression levels of TS, OPRT, and DPD in tumor sections by immunohistochemistry (Fig. 1). In the S-1 arm, intratumoral TS, OPRT, and DPD expression levels (HSCOREs) varied from 5 to 185 (median, 75), from 90 to 270 (median, 150), and from 15 to 205 (median, 105), respectively (Fig. 2). In the PTX arm, these values ranged from 0 to 170 (median, 70), from 15 to 250 (median, 120), and from 5 to 225 (median, 100), respectively. No significant difference in TS ($P = 0.54$), OPRT ($P = 0.37$), or DPD ($P = 0.28$) expression levels was apparent between the two arms. The expression level of DPD was not correlated with that of TS ($R^2 = 0.0090$, data not shown), and the expression level of OPRT was not correlated with that of TS or DPD ($R^2 = 0.0074$ and 0.11, respectively; data not shown).

We next evaluated the relation between the expression of these enzymes and the tumor response to treatment. Tumors were categorized as either responding (CR or PR) or nonresponding (stable disease [SD] or progressive disease [PD]). In the S-1 arm, the TS expression level for the responding groups (range, 5–105) was significantly ($P = 0.006$) lower than that for the nonresponding groups (range, 65–185) (Fig. 3A). In contrast, the level of TS expression did not differ significantly ($P = 0.63$) between responders and nonresponders in the PTX arm (Fig. 3A). The expression levels of OPRT (Fig. 3B) and DPD (Fig. 3C) were not significantly associated with tumor response in the S-1 arm or the PTX arm, although the expression level of DPD tended to be lower in responders than in nonresponders of the S-1 arm ($P = 0.055$).

3.3. Predictive relevance of TS and DPD expression levels in NSCLC

We performed ROC curve analysis to establish the optimal cutoff values for the HSCORE of enzyme expression level for differentiation of responders from nonresponders. Values of 55, 97.5, and 162.5 for TS, OPRT, and DPD, respectively, were obtained for the S-1 arm (Fig. 4). In patients treated with S-1 plus CBDCA, response rates were 100% (6 out of 6) and 19% (3 out of 16) for tumors with low (<55) or high (≥55) levels of TS expression ($P = 0.001$), respectively (Table 2). In contrast, there was no significant ($P = 1.0$) difference in response rate between tumors with high or low levels of TS expression in the PTX arm. In the S-1 arm, the response rate for tumors with a high level (≥162.5) of DPD expression was significantly lower than that for those with a low level (<162.5) of DPD expression (0 versus 56%, $P = 0.046$) (Table 2), whereas no such difference was observed in the PTX arm ($P = 0.52$). In the S-1 arm, the expression level of DPD was not correlated with that of TS ($R^2 = 0.046$); however, the responder in low DPD levels ($n = 9$) included all the responder in low TS levels ($n = 6$) (Fig. 5). No signif-

Please cite this article in press as: Takeda M, et al. Thymidylate synthase and dihydropyrimidine dehydrogenase expression levels are associated with response to S-1 plus carboplatin in advanced non-small cell lung cancer. Lung Cancer (2010), doi:10.1016/j.lungcan.2010.10.022

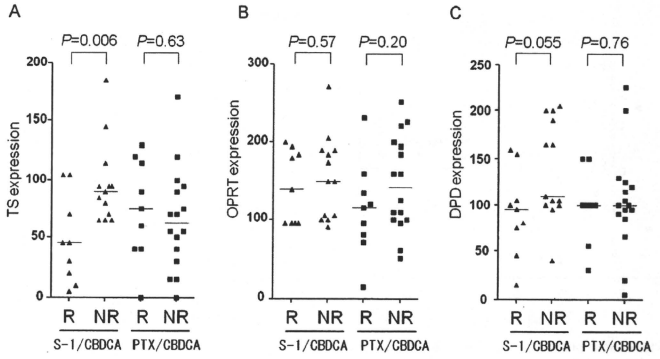

Fig. 3. Relation of expression levels of TS (A), OPRT (B), or DPD (C) in NSCLC specimens of patients treated with S-1 plus CBDCA or with PTX plus CBDCA to treatment response. NR and R represent nonresponders and responders, respectively, and median values for expression level (HSCORE) are indicated by the horizontal lines. *P* values were determined with the Mann–Whitney *U* test.

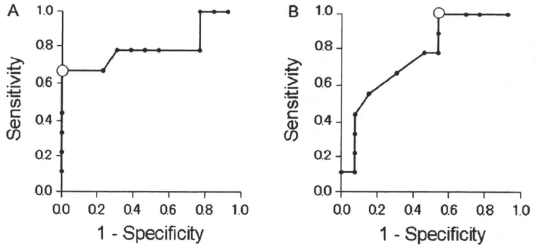

Fig. 4. Receiver operating characteristic (ROC) analysis based on intratumoral TS (A) and DPD (B) expression levels with response to S-1/CBDCA therapy. The optimal cut-off point (open circle) was 55 and 162.5 for TS and DPD, respectively, which yielded the maximum sensitivity plus specificity.

icant association between high or low OPRT expression level and response rate was apparent in either arm.

Finally, for patients treated with S-1 plus CBDCA, the progression-free survival in low TS group tended to be longer than that in high TS group, although the difference was not statistically significant ($P = 0.11$) (Fig. 6A). Patients with a low level of TS expression had a significantly ($P = 0.02$) longer overall survival than did those with a high level (Fig. 6B). In contrast, there was no significant difference in progression-free survival ($P = 0.62$) and overall survival ($P = 0.83$) between patients with a high or low level of TS expression in the PTX arm (Fig. 6C and D). Progression-free survival and overall survival for patients with a low level of DPD expression was significantly ($P = 0.013$ and 0.009, respectively; data not shown) longer than that for those with a high level in the S-1 arm, whereas no such difference ($P = 0.57$ and 0.27, respectively) was apparent in the PTX arm (data not shown). As shown in Table 3, 73% of patients with recurrence disease in the S-1 arm and 84% in the PTX arm received subsequent treatment. No bias for subsequent treatments between the two arms was observed.

4. Discussion

We have investigated the relation between intratumoral expression levels of TS, OPRT, or DPD and clinical outcome for NSCLC patients treated with S-1 plus CBDCA (S-1 arm) or with PTX plus CBDCA (PTX arm). The expression level of these proteins was assessed by immunohistochemical analysis in a semiquantitative manner by scoring the proportions of tumor cells with defined staining intensities relative to the total number of tumor cells. ROC curves are commonly used to determine biologically or clinically

Table 2
Tumor response to treatment according to TS or DPD expression level. All *P* values were determined with Fisher's exact test.

Relative expression level	S-1 plus CBDCA ($n = 22$)			PTX plus CBDCA ($n = 25$)		
	Responders*n* (%)	Nonresponders*n* (%)	*P*	Responders*n* (%)	Nonresponders*n* (%)	*P*
High TS	3 (19)	13 (81)	0.001	6 (38)	10 (63)	1.0
Low TS	6 (100)	0 (0)		3 (33)	6 (67)	
High DPD	0 (0)	6 (100)	0.046	0 (0)	2 (100)	0.52
Low DPD	9 (56)	7 (44)		9 (39)	14 (61)	

Please cite this article in press as: Takeda M, et al. Thymidylate synthase and dihydropyrimidine dehydrogenase expression levels are associated with response to S-1 plus carboplatin in advanced non-small cell lung cancer. Lung Cancer (2010), doi:10.1016/j.lungcan.2010.10.022

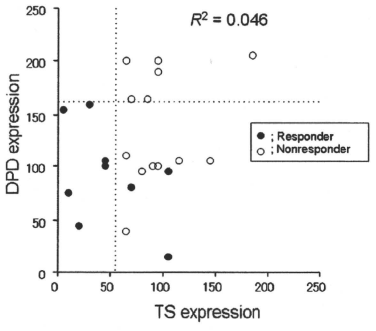

Fig. 5. Correlation between TS and DPD expression levels in patients treated with S-1 plus CBDCA. The dotted lines indicate the optimal cutoff values for the HSCORE of each expression level. The closed circles represent the responder, and the open circles represent the nonresponder.

relevant cutoff scores in such analysis [12,13], and we therefore used ROC curves to define the optimal cutoff values of TS or DPD expression level (HSCORE) for discrimination of responders from nonresponders in the S-1 arm. We found that low levels of TS and DPD expression were associated with a better treatment response and a longer survival time in NSCLC patients in the S-1 arm. To examine the predictive or prognostic relevance of the cutoff values for TS or DPD expression level determined in the S-1 arm, we applied these values to the results obtained for patients treated with PTX plus CBDCA, which is a standard first-line chemotherapy regimen for advanced NSCLC. Neither the expression of TS nor that of DPD showed a significant association with treatment response or survival in the PTX arm. These results thus indicate that the expression levels of TS and DPD are independent predictive markers, rather than prognostic markers, in patients with advanced NSCLC receiving S-1-based chemotherapy.

Table 3
Treatment after recurrence in each arm.

Variable	Treatment arm		*P*
	S-1 plus CBDCA *n* (%)	PTX plus CBDCA *n* (%)	
Any treatment	16 (73)	21 (84)	0.48
Radiotherapy	3 (14)	4 (16)	1.00
Any chemotherapy	11 (50)	17 (68)	0.25
Docetaxel	5 (23)	9 (36)	0.36
Gefitinib	3 (14)	8 (32)	0.18

TS is an essential enzyme that catalyzes the transfer of a methyl group from methylenetetrahydrofolate to dUMP in order to generate dTMP [14,15]. The subsequent phosphorylation of dTMP to dTTP provides a direct precursor for DNA synthesis. Several in vitro studies with tumor cell lines have implicated up-regulation of TS expression as a mechanism of resistance to 5-FU that develops after exposure to the drug [16–19]. Previous clinical studies have also shown that a low level of TS expression was associated with high sensitivity to 5-FU, to 5-FU plus cisplatin, or to 5-FU plus methotrexate in colorectal or gastric cancer [11]. A low level of TS expression in NSCLC tumors has also been associated with longer survival in patients treated with oral 5-FU–based agents after curative resection [20–22]. S-1 is an oral fluoropyrimidine derivative

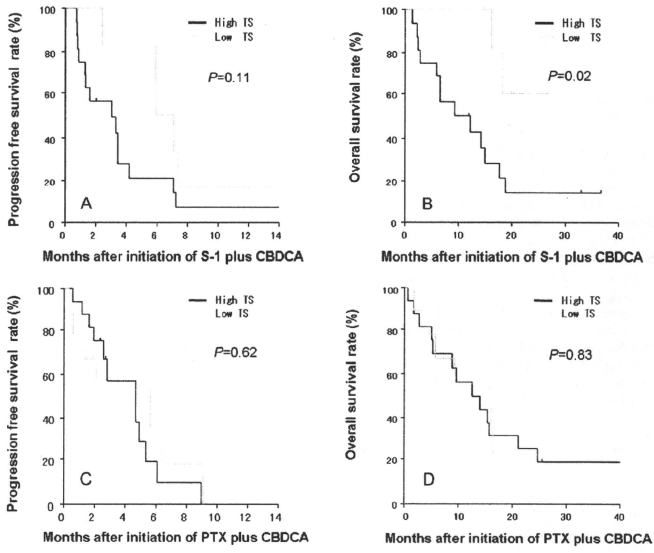

Fig. 6. Progression-free survival and overall survival according to expression level of TS in NSCLC tumors of patients treated with S-1 plus CBDCA (A and B) or with PTX plus CBDCA (C and D). *P* values were determined with the log-rank test.

Please cite this article in press as: Takeda M, et al. Thymidylate synthase and dihydropyrimidine dehydrogenase expression levels are associated with response to S-1 plus carboplatin in advanced non-small cell lung cancer. Lung Cancer (2010), doi:10.1016/j.lungcan.2010.10.022

that contains the 5-FU prodrug tegafur, and it is therefore expected to have an antitumor effect in patients with tumors sensitive to 5-FU. Indeed, low levels of TS expression in gastric cancer have been linked to a favorable clinical outcome after S-1 treatment [23–25]. However, the relation between TS status and tumor response to S-1 or to S-1 combination therapy has not previously been examined for NSCLC. We have now shown that a low level of TS expression was significantly associated with response to treatment with S-1 plus CBDCA in patients with advanced NSCLC.

DPD is an initial and rate-limiting enzyme in the catabolism of 5-FU, with >80% of 5-FU being degraded to inactive metabolites by this enzyme in human tissues, and DPD activity therefore modulates the antitumor effects of 5-FU. In vitro studies have shown that overexpression of DPD in cancer cell lines confers resistance to 5-FU [16,26]. Several clinical studies have also shown that a high level of DPD expression in tumors was associated with poor survival in NSCLC patients treated with oral 5-FU-based agents after curative surgery [20,21,27,28], whereas a relation between DPD expression level and clinical outcome after 5-FU treatment has not been definitively demonstrated for colorectal or gastric cancer [11]. S-1 contains CDHP, an inhibitor of DPD, and an antitumor effect of S-1 is therefore expected even in tumors with a high level of DPD activity. Indeed, patients with gastric cancer expressing DPD at high levels were found to benefit from S-1 treatment [23–25]. No previous studies have evaluated the relation between DPD expression and S-1 sensitivity in NSCLC, however. We have now shown that a high level of DPD expression in NSCLC predicts resistance to S-1-based chemotherapy. DPD activity levels have been shown to be higher in NSCLC tissue than in other solid tumors including gastric, colorectal, and breast cancer [29]. The apparent discrepancy between the demonstrated clinical efficacy of S-1 in patients with gastric cancer expressing DPD at high levels [23–25] and our finding that no NSCLC patients with a high level of DPD expression responded to treatment with S-1 plus CBDCA may be attributable to the fact that DPD activity levels in NSCLC tissue are about twice those in gastric cancer [29]. In cancers with a high level of DPD expression, such as NSCLC, the amount of the free enzyme may be maintained in excess of that of the CDHP-bound enzyme.

Molecular targeting therapies have been developed as a new strategy for the treatment of advanced NSCLC, and somatic mutations in the epidermal growth factor receptor (*EGFR*) gene are the most robust biomarker for EGFR tyrosine kinase inhibitor (TKI) therapy in NSCLC. A recent study has reported that *EGFR* mutant tumors have a lower sensitivity to another oral 5-FU derivative, uracil-tegafur, than that of *EGFR* wild-type tumors [30]. We have previously shown that EGFR-TKI-induced downregulation of TS is responsible for the enhanced antitumor effect of combined treatment with S-1 [31–33]. Based on these results, further studies are warranted to investigate the relationship between the presence of *EGFR* mutation and TS/DPD expression levels in NSCLC.

In conclusion, we have shown that the tumor expression levels of TS and DPD were predictive of tumor response to S-1-based chemotherapy in patients with advanced NSCLC. S-1 in combination with platinum compounds (cisplatin or CBDCA) is currently under evaluation as a first-line treatment for advanced NSCLC in randomized phase III studies. It will be necessary to confirm that the expression levels of TS and DPD can predict clinical outcome in these clinical trials, given that our findings derive from a limited retrospective study of a relatively small number of patients. Further prospective studies of these biomarkers are also needed to address the issue of reproducibility in a large series of patients.

Conflict of interest statement

The authors declare no conflict of interest.

Acknowledgments

We thank Yoshihiro Okayama and Hirofumi Hagimoto for technical assistance.

References

[1] Hoffman PC, Mauer AM, Vokes EE. Lung cancer. Lancet 2000;355:479–85.
[2] Schiller JH, Harrington D, Belani CP, Langer C, Sandler A, Krook J, et al. Comparison of four chemotherapy regimens for advanced non-small-cell lung cancer. N Engl J Med 2002;346:92–8.
[3] Olaussen KA, Dunant A, Fouret P, Brambilla E, Andre F, Haddad V, et al. DNA repair by ERCC1 in non-small-cell lung cancer and cisplatin-based adjuvant chemotherapy. N Engl J Med 2006;355:983–91.
[4] Taron M, Rosell R, Felip E, Mendez P, Souglakos J, Ronco MS, et al. BRCA1 mRNA expression levels as an indicator of chemoresistance in lung cancer. Hum Mol Genet 2004;13:2443–9.
[5] Reynolds C, Obasaju C, Schell MJ, Li X, Zheng Z, Boulware D, et al. Randomized phase III trial of gemcitabine-based chemotherapy with in situ RRM1 and ERCC1 protein levels for response prediction in non-small-cell lung cancer. J Clin Oncol 2009;27:5808–15.
[6] Okamoto I, Nishimura T, Miyazaki M, Yoshioka H, Kubo A, Takeda K, et al. Phase II study of combination therapy with S-1 and irinotecan for advanced non-small cell lung cancer: west Japan thoracic oncology group 3505. Clin Cancer Res 2008;14:5250–4.
[7] Tamura K, Okamoto I, Ozaki T, Kashii T, Takeda K, Kobayashi M, et al. Phase I/II study of S-1 plus carboplatin in patients with advanced non-small cell lung cancer. Eur J Cancer 2009;45:2132–7.
[8] Kaira K, Sunaga N, Yanagitani N, Imai H, Utsugi M, Shimizu Y, et al. A phase I dose-escalation study of S-1 plus carboplatin in patients with advanced non-small-cell lung cancer. Anticancer Drugs 2007;18:471–6.
[9] Kubota K, Sakai H, Yamamoto N, Kunitoh H, Nakagawa K, Takeda K, et al. A multi-institution phase I/II trial of triweekly regimen with S-1 plus cisplatin in patients with advanced non-small cell lung cancer. J Thorac Oncol 2010;5:702–6.
[10] Okamoto I, Fukuoka M. S-1: a new oral fluoropyrimidine in the treatment of patients with advanced non-small-cell lung cancer. Clin Lung Cancer 2009;10:290–4.
[11] Maring JG, Groen HJ, Wachters FM, Uges DR, de Vries EG. Genetic factors influencing pyrimidine-antagonist chemotherapy. Pharmacogenomics J 2005;5:226–43.
[12] Zlobec I, Steele R, Terracciano L, Jass JR, Lugli A. Selecting immunohistochemical cut-off scores for novel biomarkers of progression and survival in colorectal cancer. J Clin Pathol 2007;60:1112–6.
[13] Zlobec I, Vuong T, Hayashi S, Haegert D, Tornillo L, Terracciano L, et al. A simple and reproducible scoring system for EGFR in colorectal cancer: application to prognosis and prediction of response to preoperative brachytherapy. Br J Cancer 2007;96:793–800.
[14] Danenberg PV. Thymidylate synthetase—a target enzyme in cancer chemotherapy. Biochim Biophys Acta 1977;473:73–92.
[15] Johnston PG, Lenz HJ, Leichman CG, Danenberg KD, Allegra CJ, Danenberg PV, et al. Thymidylate synthase gene and protein expression correlate and are associated with response to 5-fluorouracil in human colorectal and gastric tumors. Cancer Res 1995;55:1407–12.
[16] Kirihara Y, Yamamoto W, Toge T, Nishiyama M. Dihydropyrimidine dehydrogenase, multidrug resistance-associated protein, and thymidylate synthase gene expression levels can predict 5-fluorouracil resistance in human gastrointestinal cancer cells. Int J Oncol 1999;14:551–6.
[17] Fukushima M, Fujioka A, Uchida J, Nakagawa F, Takechi T. Thymidylate synthase (TS) and ribonucleotide reductase (RNR) may be involved in acquired resistance to 5-fluorouracil (5-FU) in human cancer xenografts in vivo. Eur J Cancer 2001;37:1681–7.
[18] Copur S, Aiba K, Drake JC, Allegra CJ, Chu E. Thymidylate synthase gene amplification in human colon cancer cell lines resistant to 5-fluorouracil. Biochem Pharmacol 1995;49:1419–26.
[19] Matsuoka K, Tsukuda K, Suda M, Kobayashi K, Ota T, Okita A, et al. The transfection of thymidylate synthase antisense suppresses oncogenic properties of a human colon cancer cell line and augments the antitumor effect of fluorouracil. Int J Oncol 2004;24:217–22.
[20] Nakano J, Huang C, Liu D, Masuya D, Nakashima T, Yokomise H, et al. Evaluations of biomarkers associated with 5-FU sensitivity for non-small-cell lung cancer patients postoperatively treated with UFT. Br J Cancer 2006;95:607–15.
[21] Huang CL, Yokomise H, Kobayashi S, Fukushima M, Hitomi S, Wada H. Intratumoral expression of thymidylate synthase and dihydropyrimidine dehydrogenase in non-small cell lung cancer patients treated with 5-FU-based chemotherapy. Int J Oncol 2000;17:47–54.
[22] Miyoshi T, Kondo K, Toba H, Yoshida M, Fujino H, Kenzaki K, et al. Predictive value of thymidylate synthase and dihydropyrimidine dehydrogenase expression in tumor tissue, regarding the efficacy of postoperatively administered UFT (tegafur + uracil) in patients with non-small cell lung cancer. Anticancer Res 2007;27:2641–8.
[23] Ichikawa W, Takahashi T, Suto K, Yamashita T, Nihei Z, Shirota Y, et al. Thymidylate synthase predictive power is overcome by irinotecan combination therapy with S-1 for gastric cancer. Br J Cancer 2004;91:1245–50.

Please cite this article in press as: Takeda M, et al. Thymidylate synthase and dihydropyrimidine dehydrogenase expression levels are associated with response to S-1 plus carboplatin in advanced non-small cell lung cancer. Lung Cancer (2010), doi:10.1016/j.lungcan.2010.10.022

[24] Ichikawa W, Takahashi T, Suto K, Shirota Y, Nihei Z, Shimizu M, et al. Simple combinations of 5-FU pathway genes predict the outcome of metastatic gastric cancer patients treated by S-1. Int J Cancer 2006;119:1927–33.
[25] Matsubara J, Nishina T, Yamada Y, Moriwaki T, Shimoda T, Kajiwara T, et al. Impacts of excision repair cross-complementing gene 1 (ERCC1), dihydropyrimidine dehydrogenase, and epidermal growth factor receptor on the outcomes of patients with advanced gastric cancer. Br J Cancer 2008;98:832–9.
[26] Beck A, Etienne MC, Cheradame S, Fischel JL, Formento P, Renee N, et al. A role for dihydropyrimidine dehydrogenase and thymidylate synthase in tumour sensitivity to fluorouracil. Eur J Cancer 1994;30A:1517–22.
[27] Shintani Y, Ohta M, Hirabayashi H, Tanaka H, Iuchi K, Nakagawa K, et al. Thymidylate synthase and dihydropyrimidine dehydrogenase mRNA levels in tumor tissues and the efficacy of 5-fluorouracil in patients with non-small-cell lung cancer. Lung Cancer 2004;45:189–96.
[28] Nakagawa T, Tanaka F, Takata T, Matsuoka K, Miyahara R, Otake Y, et al. Predictive value of dihydropyrimidine dehydrogenase expression in tumor tissue, regarding the efficacy of postoperatively administered UFT (tegafur + uracil) in patients with p-stage I nonsmall-cell lung cancer. J Surg Oncol 2002;81:87–92.
[29] Fukushima M, Morita M, Ikeda K, Nagayama S. Population study of expression of thymidylate synthase and dihydropyrimidine dehydrogenase in patients with solid tumors. Int J Mol Med 2003;12:839–44.
[30] Suehisa H, Toyooka S, Hotta K, Uchida A, Soh J, Fujiwara Y, et al. Epidermal growth factor receptor mutation status and adjuvant chemotherapy with uracil-tegafur for adenocarcinoma of the lung. J Clin Oncol 2007;25:3952–7.
[31] Okabe T, Okamoto I, Tsukioka S, Uchida J, Hatashita E, Yamada Y, et al. Addition of S-1 to the epidermal growth factor receptor inhibitor gefitinib overcomes gefitinib resistance in non-small cell lung cancer cell lines with MET amplification. Clin Cancer Res 2009;15:907–13.
[32] Okabe T, Okamoto I, Tsukioka S, Uchida J, Iwasa T, Yoshida T, et al. Synergistic antitumor effect of S-1 and the epidermal growth factor receptor inhibitor gefitinib in non-small cell lung cancer cell lines: role of gefitinib-induced downregulation of thymidylate synthase. Mol Cancer Ther 2008;7:599–606.
[33] Takezawa K, Okamoto I, Tanizaki J, Kuwata K, Yamaguchi H, Fukuoka M, et al. Enhanced anticancer effect of the combination of BIBW2992 and thymidylate synthase-targeted agents in non-small cell lung cancer with the T790M mutation of epidermal growth factor receptor. Mol Cancer Ther 2010;9:1647–56.

Please cite this article in press as: Takeda M, et al. Thymidylate synthase and dihydropyrimidine dehydrogenase expression levels are associated with response to S-1 plus carboplatin in advanced non-small cell lung cancer. Lung Cancer (2010), doi:10.1016/j.lungcan.2010.10.022

British Journal of Cancer (2011) 104, 1594 – 1601

www.bjcancer.com

Thymidylate synthase as a determinant of pemetrexed sensitivity in non-small cell lung cancer

K Takezawa[1], I Okamoto*,[1], W Okamoto[1], M Takeda[1], K Sakai[2], S Tsukioka[3], K Kuwata[1], H Yamaguchi[1], K Nishio[2] and K Nakagawa[1]

[1]Department of Medical Oncology, Kinki University Faculty of Medicine, 377-2 Ohno-higashi, Osaka-Sayama, Osaka 589-8511, Japan; [2]Department of Genome Biology, Kinki University Faculty of Medicine, 377-2 Ohno-higashi, Osaka-Sayama, Osaka 589-8511, Japan; [3]Tokushima Research Center, Taiho Pharmaceutical Co. Ltd., 224-2 Hiraishi-ebisuno, Kawauchi, Tokushima 771-0194, Japan

BACKGROUND: Although a high level of thymidylate synthase (TS) expression in malignant tumours has been suggested to be related to a reduced sensitivity to the antifolate drug pemetrexed, no direct evidence for such an association has been demonstrated in non-small cell lung cancer (NSCLC). We have now investigated the effect of TS overexpression on pemetrexed sensitivity in NSCLC cells.
METHODS: We established NSCLC cell lines that stably overexpress TS and examined the effects of such overexpression on the cytotoxicity of pemetrexed both *in vitro* and in xenograft models. We further examined the relation between TS expression in tumour specimens from NSCLC patients and the tumour response to pemetrexed by immunohistochemical analysis.
RESULTS: The sensitivity of NSCLC cells overexpressing TS to the antiproliferative effect of pemetrexed was markedly reduced compared with that of control cells. The inhibition of DNA synthesis and induction of apoptosis by pemetrexed were also greatly attenuated by forced expression of TS. Furthermore, tumours formed by TS-overexpressing NSCLC cells in nude mice were resistant to the growth-inhibitory effect of pemetrexed observed with control tumours. Finally, the level of TS expression in tumours of non-responding patients was significantly higher than that in those of responders, suggestive of an inverse correlation between TS expression and tumour response to pemetrexed.
CONCLUSION: A high level of TS expression confers a reduced sensitivity to pemetrexed. TS expression is thus a potential predictive marker for response to pemetrexed-based chemotherapy in NSCLC patients.
British Journal of Cancer (2011) **104,** 1594 – 1601. doi:10.1038/bjc.2011.129 www.bjcancer.com
Published online 12 April 2011

Keywords: non-small cell lung cancer; thymidylate synthase; pemetrexed; apoptosis; immunohistochemistry

Lung cancer is the most common cause of cancer-related death worldwide, with non-small cell lung cancer (NSCLC) accounting for ~75% of all lung cancer cases (Hoffman *et al*, 2000). Platinum-based chemotherapy is the standard first-line treatment for individuals with advanced NSCLC, but the efficacy of such agents with regard to improving clinical outcome is limited (Schiller *et al*, 2002). Both experimental and clinical studies have revealed that many molecules contribute to the biological activities of malignant tumours including NSCLC. New strategies based on a better understanding of tumour biology may thus help to maximise the efficacy of current treatments.

A relatively new antifolate drug, pemetrexed, inhibits the growth of a variety of tumour types by targeting multiple folate-dependent enzymes including thymidylate synthase (TS), dihydrofolate reductase, and glycinamide ribonucleotide formyltransferase (Shih *et al*, 1997). The antitumour efficacy of pemetrexed has been found to be more limited in lung cancer patients with squamous cell carcinoma than in those with other histotypes of NSCLC (Scagliotti *et al*, 2008). Furthermore, the abundance of TS mRNA or protein seems to be higher in squamous cell carcinoma than in other histotypes of NSCLC (Ceppi *et al*, 2006; Monica *et al*, 2009; Takezawa *et al*, 2010), and high levels of TS expression in various tumour types have been suggested to correlate with a poor response to TS-targeted agents (Johnston *et al*, 1994, 1997; Pestalozzi *et al*, 1997; Ferguson *et al*, 1999). The poorer response of NSCLC patients with squamous cell carcinoma to pemetrexed is thus thought to result from the higher level of TS expression in such tumours. However, such a relation between a high TS expression level and a reduced sensitivity to pemetrexed in NSCLC has not been well established. Moreover, the precise mechanism that might underlie a reduced sensitivity to pemetrexed in tumours with a high level of TS expression remains unknown.

We have now constructed an expression vector for TS and have used this vector to establish several NSCLC cell lines that stably overexpress TS. With the use of these cells, we examined the relation between the anticancer effects of pemetrexed both *in vitro* and *in vivo* and the expression level of TS. We further investigated the relation between pemetrexed sensitivity and TS expression level in primary lung cancer patients.

MATERIALS AND METHODS

Cell culture and reagents

The human lung cancer cell lines A549, H1299, and PC9 were obtained from American Type Culture Collection (Manassas, VA, USA).

*Correspondence: Dr I Okamoto;
E-mail: chi-okamoto@dotd.med.kindai.ac.jp
Revised 9 March 2011; accepted 21 March 2011; published online 12 April 2011

All cells were cultured in RPMI 1640 medium (Sigma, St Louis, MO, USA) supplemented with 10% fetal bovine serum and 1% penicillin-streptomycin (Sigma), and they were maintained under a humidified atmosphere of 5% CO_2 at 37°C. Pemetrexed, cisplatin, and docetaxel were obtained from Wako (Osaka, Japan).

Generation of TS-overexpressing NSCLC cell lines

A full-length cDNA fragment encoding TS was obtained from PC9 cells by reverse transcription and the polymerase chain reaction with the primers TS-F (5′-AAGCTTCGCGCCATGCCTGTGG CCGGCTCGGAG-3′) and TS-R (5′-GCGGCCGCCTAAACAGCC ATTTCCATTTTAATAG-3′). The amplification product was verified by sequencing after its cloning into the pCR-Blunt II-TOPO vector (Invitrogen, Carlsbad, CA, USA). The TS cDNA was excised from pCR-Blunt II-TOPO and transferred to the pMZs retroviral vector (Cell Biolabs, San Diego, CA, USA). The resulting pMZs construct and the pVSV-G vector (Clontech, Palo Alto, CA, USA) for construction of the viral envelope were introduced into GP2-293 cells (~80% confluence in a 10-cm dish) with the use of the FuGENE6 transfection reagent. After 48 h, the viral particles released into the culture medium were concentrated by centrifugation at 15 000 × **g** for 3 h at 4°C. The resulting pellet was then suspended in fresh RPMI 1640 medium and used to infect A549, H1299, or PC9 cells as previously described (Okamoto *et al*, 2010).

Immunoblot analysis

Cells were washed twice with ice-cold phosphate-buffered saline (PBS) and then lysed in a solution containing 20 mM Tris-HCl (pH 7.5), 150 mM NaCl, 1 mM EDTA, 1% Triton X-100, 2.5 mM sodium pyrophosphate, 1 mM phenylmethylsulfonyl fluoride, and leupeptin (1 $\mu g\,ml^{-1}$). The protein concentration of cell lysates was determined with the Bradford reagent (Bio-Rad, Hercules, CA, USA), and equal amounts of lysate protein were subjected to SDS-polyacrylamide gel electrophoresis on a 7.5 or 12% gel. The separated proteins were transferred to a nitrocellulose membrane, which was then exposed to 5% non-fat dried milk in PBS for 1 h at room temperature before incubation overnight at 4°C with primary antibodies. Rabbit polyclonal antibodies to human TS were obtained from Santa Cruz Biotechnology (Santa Cruz, CA, USA), and those to β-actin were from Sigma. The membrane was then washed with PBS containing 0.05% Tween 20 before incubation for 1 h at room temperature with horseradish peroxidase-conjugated goat antibodies to rabbit immunoglobulin G (Sigma). Immune complexes were finally detected with chemiluminescence reagents (GE Healthcare, Little Chalfont, UK).

Assay of TS activity

Thymidylate synthase activity was quantified with the use of a tritiated 5-fluoro-dUMP binding assay. Cells were harvested, diluted in 0.2 M Tris-HCl (pH 7.4) containing 20 mM 2-mercaptoethanol, 15 mM CMP, and 100 mM NaF, and disrupted by ultrasonic treatment. The cell lysate was centrifuged at 1600 × **g** for 15 min at 4°C, and the resulting supernatant was centrifuged at 105 000 × **g** for 1 h at 4°C. A portion (50 μl) of the final supernatant was mixed consecutively with 50 μl of Buffer A (600 mM NH_4HCO_3 buffer (pH 8.0), 100 mM 2-mercaptoethanol, 100 mM NaF, 15 mM CMP) and with 50 μl of (6-^{3}H)5-fluoro-dUMP (7.8 pmol) plus 25 μl of cofactor solution (50 mM potassium phosphate buffer (pH 7.4), 20 mM 2-mercaptoethanol, 100 mM NaF, 15 mM CMP, 2% bovine serum albumin, 2 mM tetrahydrofolic acid, 16 mM sodium ascorbate, 9 mM formaldehyde). The resulting mixture was incubated at 30°C for 20 min, after which the reaction was terminated by the addition of 100 μl of 2% bovine serum albumin and 275 μl of 1 M $HClO_4$ and by centrifugation at 1600 × **g** for 15 min at 4°C. The resulting precipitate was suspended in 2 ml of 0.5 M $HClO_4$, and the mixture was subjected to ultrasonic treatment followed by centrifugation at 1600 × **g** for 15 min at 4°C. The final precipitate was solubilised with 0.5 ml of 98% formic acid, mixed with 10 ml of ACS II scintillation fluid, and assayed for radioactivity. Data are expressed as picomoles of substrate consumed per milligram of soluble protein.

Cell growth inhibition assay *in vitro* (MTT assay)

Cells were plated in 96-well flat-bottomed plates and cultured for 24 h before exposure to various concentrations of drugs for 72 h. TetraColor One (5 mM tetrazolium monosodium salt and 0.2 mM 1-methoxy-5-methyl phenazinium methylsulfate; Seikagaku, Tokyo, Japan) was then added to each well, and the cells were incubated for 3 h at 37°C before measurement of absorbance at 490 nm with a Multiskan Spectrum instrument (Thermo Labsystems, Boston, MA, USA).

RNA interference

Cells were plated at 50–60% confluence in six-well plates or 25-cm^2 flasks and then incubated for 24 h before transient transfection for the indicated times with small interfering RNAs (siRNAs) mixed with the Lipofectamine reagent (Invitrogen). An siRNA specific for human TS mRNA (5′-CAAUCCGCAUCCAA CUAUU-3′) and a nonspecific siRNA (5′-GUUGAGAGAUAUUA GAGUU-3′) was obtained from Nippon EGT (Toyama, Japan).

Assay of DNA synthesis

DNA synthesis was measured with the use of a Cell Proliferation ELISA BrdU Kit (Roche, Basel, Switzerland). In brief, cells were seeded in 96-well plates at a density of 10 000–20 000 per well and exposed to various concentrations of drugs for 48 h. They were then incubated in the additional presence of bromodeoxyuridine (BrdU) for 3 h before exposure to detection reagents for 15 min at 25°C and measurement of luminescence.

Annexin V binding assay

Binding of annexin V to cells was measured with the use of an Annexin-V-FLUOS Staining Kit (Roche). Cells were harvested by exposure to trypsin–EDTA, washed with PBS, and centrifuged at 200 × **g** for 5 min. The cell pellets were resuspended in 100 μl of Annexin-V-FLUOS labelling solution, incubated for 10–15 min at 15 to 25°C, and then analysed for fluorescence with a flow cytometer (FACS Calibur) (Becton Dickinson, San Jose, CA, USA) and Cell Quest software (Becton Dickinson).

Animals

Male athymic nude mice were maintained on a 12-h light, 12-h dark cycle and provided with food and water ad libitum in a barrier facility. All animal experiments were carried out with approval of the institutional animal care and use committee and complied with the specifications of the Association for Assessment and Accreditation of Laboratory Animal Care of Japan.

Tumour growth inhibition assay *in vivo*

Cubic fragments of tumour tissue (~2 by 2 by 2 mm) were implanted subcutaneously into the axilla of 5- to 6-week-old male athymic nude mice. Treatment was initiated when tumours in each group of eight mice achieved an average volume of 150–200 mm^3. Pemetrexed (100 mg per kilogram of body weight) or vehicle (physiological saline) was administered intraperitoneally once a week. Tumour volume was determined from caliper measurements of tumour length (L) and width (W) according to the formula $LW^2/2$. Both tumour size and body weight were measured twice per week.

Patients and clinical specimens

For retrospective analysis, we recruited consecutive patients with advanced NSCLC who received chemotherapy at Kinki University Hospital between April 2008 and June 2010. Patients met all of the following criteria: a histological diagnosis of NSCLC with at least one measurable lesion; a clinical stage of 3B or 4; an Eastern Cooperative Oncology Group (ECOG) performance status of 0 or 1; adequate haematologic, hepatic, and renal function; treatment either with carboplatin at an area under the curve (AUC) of 5 on day 1 and pemetrexed at 500 mg m^{-2} on day 1 of an 21-day cycle or with cisplatin at 75 mg m^{-2} on day 1 and pemetrexed at 500 mg m^{-2} on day 1 of an 21-day cycle as first-line chemotherapy; and availability of sufficient tumour tissue in paraffin blocks for assessment by immunohistochemistry. Tumour tissue specimens were obtained by transbronchial lung biopsy. Tumour response was examined by computed tomography and evaluated according to the Response Evaluation Criteria in Solid tumours (RECIST) as complete response (CR), partial response (PR), stable disease (SD), or progressive disease (PD). This study conforms to the provisions of the Declaration of Helsinki and was approved by the local institutional review board.

Immunohistochemistry and scoring of TS expression

Paraffin-embedded sections (thickness, 4 μm) of tumour tissue were depleted of paraffin with xylene and then rehydrated, and endogenous peroxidase activity was quenched by incubation with 0.3% hydrogen peroxide in methanol. Antigen retrieval was carried out by microwave irradiation for 10 min in citrate buffer (pH 6.0). The sections were then washed with PBS before incubation overnight at room temperature with rabbit polyclonal antibodies to TS (Taiho Pharmaceutical Co., Saitama, Japan) at a dilution of 1 : 100. Immune complexes were detected by incubation at room temperature for 30 min first with biotinylated goat antibodies to rabbit immunoglobulin G (Dako, Santa Barbara, CA, USA) and then with streptavidin-conjugated horseradish peroxidase (Dako). Peroxidase activity was visualised with diaminobenzidine tetrahydrochloride solution (Dako), and the sections were counter-stained with hematoxylin before examination with a microscope (Dako). The human colon cancer cell line DLD-1/FrUrd, human breast cancer cell line MDA-MB-435S, and human pancreatic cancer cell line MIAPaCa-2 (all obtained from American Type Culture Collection) were used as positive controls for TS staining. All immunostained sections were reviewed by two observers without knowledge of the patients' characteristics. Sections with discrepant results were jointly reevaluated until a consensus was reached. Cytoplasmic staining for TS was scored in a semiquantitative manner, reflecting both the intensity of staining and the percentage of cells with staining at each intensity. Staining intensity was classified as 0 (no staining), +1 (weak staining), +2 (distinct staining), or +3 (strong staining). A value designated the HSCORE was obtained as $\Sigma(I \times PC)$, where I and

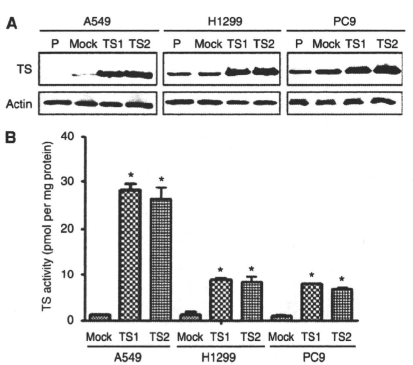

Figure 1 Abundance and enzymatic activity of TS in TS-overexpressing NSCLC cell lines. Parental (P) A549, H1299, or PC9 cells or corresponding sublines either stably overexpressing TS (TS1 and TS2) or harbouring the empty vector (Mock) were cultured overnight in complete medium, after which cell lysates were prepared and either subjected to immunoblot analysis with antibodies to TS and to β-actin (loading control) (**A**) or assayed for TS activity. (**B**) Data are means ± s.d. of triplicates from experiments that were repeated on two additional occasions with similar results. *$P < 0.05$ *vs* the corresponding value for Mock cells (Student's two-tailed *t*-test).

Table 1 Median inhibitory concentrations (μM) for the antiproliferative effects of chemotherapeutic agents in TS-overexpressing NSCLC cells *in vitro*

Cell line	Pemetrexed	Cisplatin	Docetaxel
A549/Mock	0.07	2.62	0.12
A549/TS1	0.38	2.37	0.12
A549/TS2	0.44	2.21	0.13
H1299/Mock	0.08	2.93	0.32
H1299/TS1	0.22	2.98	0.30
H1299/TS2	0.22	2.90	0.30
PC9/Mock	0.03	0.72	0.18
PC9/TS1	0.11	0.72	0.18
PC9/TS2	0.10	0.65	0.17

Abbreviations: NSCLC = non-small cell lung cancer; TS = thymidylate synthase.

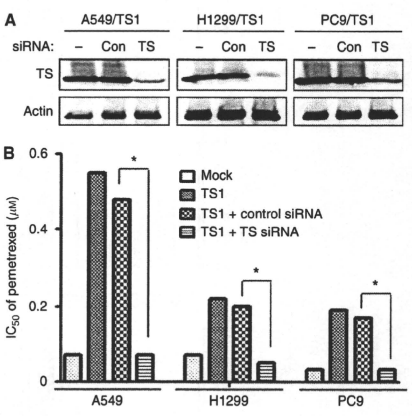

Figure 2 Effect of TS depletion on pemetrexed sensitivity in TS-overexpressing NSCLC cells. (**A**) Cells of the indicated lines were transfected or not (–) with nonspecific (Con) or TS siRNAs for 48 h, after which cell lysates were subjected to immunoblot analysis with antibodies to TS and to β-actin. (**B**) Cells transfected as in **A** were cultured for 72 h in complete medium containing various concentrations of pemetrexed, after which cell viability was assessed as described in Materials and methods section, and the median inhibitory concentration (IC_{50}) of pemetrexed was determined. Data are means of triplicates from experiments that were repeated on two additional occasions with similar results. *$P < 0.05$ (Student's two-tailed *t*-test).

PC represent staining intensity and the percentage of cells that stain at each intensity, respectively. The selection of a clinically important cutoff score for TS expression was based on receiver operating characteristic (ROC) curve analysis.

Statistical analysis

Quantitative data are presented as means ± s.d. or ± s.e.m. as indicated, and were analysed by Student's two-tailed *t*-test. Progression-free survival was assessed from the first day of chemotherapy administration to the date of objective disease progression. Kaplan–Meier analysis was used to estimate the probability of survival as a function of time, and differences in the survival of subgroups of patients were evaluated with the log-rank test. A *P*-value of <0.05 was considered statistically significant.

RESULTS

Forced expression of TS reduces the sensitivity of NSCLC cells to pemetrexed

To investigate whether the level of TS expression affects the sensitivity of NSCLC cells to pemetrexed, we first established A549 (A549/TS1 and A549/TS2), H1299 (H1299/TS1 and H1299/TS2), and PC9 (PC9/TS1 and PC9/TS2) cells that stably overexpress TS. Cells that stably harbour the corresponding empty vector (A549/Mock, H1299/Mock, and PC9/Mock) were established as controls. Immunoblot analysis showed that the abundance of TS was markedly increased in the TS-overexpressing lines compared with the parental or Mock cells (Figure 1A). The enzymatic activity of TS was also substantially higher in the TS-overexpressing cells than in the parental or Mock cells (Figure 1B). We then examined the effect of forced expression of TS on the cytotoxicity of anticancer drugs as determined with the MTT assay. The median inhibitory concentration of pemetrexed for the TS-overexpressing cells was about three to six times that for the corresponding Mock cells for all three lung cancer lines, whereas cisplatin and docetaxel inhibited the growth of the TS-overexpressing cells in a manner similar to that observed with the corresponding Mock cells (Table 1). To exclude the possibility that these results were because of nonspecific effects of transfection, we depleted A549/TS1, H1299/TS1, and PC9/TS1 cells of TS by RNA interference. Immunoblot analysis revealed that transfection of these cells with an siRNA specific for TS mRNA resulted in downregulation of the corresponding protein (Figure 2A). This reduction in the abundance of TS restored the sensitivity of the cells to the

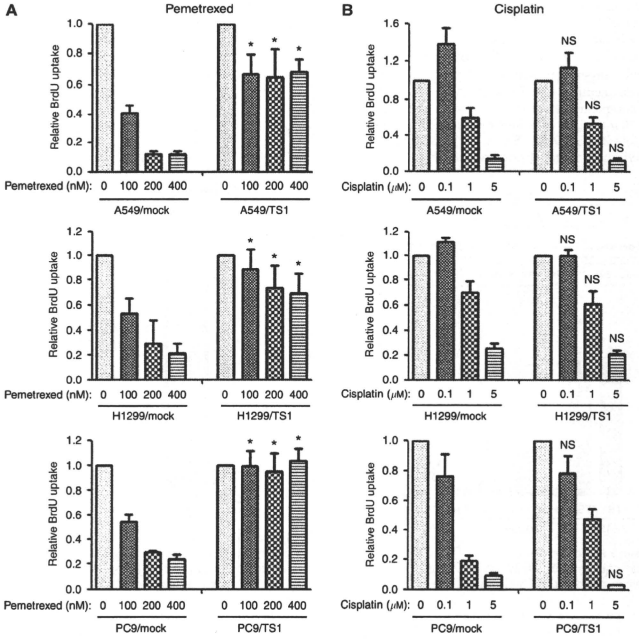

Figure 3 Effects of pemetrexed and cisplatin on DNA synthesis in NSCLC cells overexpressing TS. The indicated NSCLC cell lines were cultured for 48 h in complete medium containing various concentrations of pemetrexed (**A**) or cisplatin (**B**), after which BrdU incorporation was assessed as described in Materials and methods section. Data are means ± s.d. of triplicates from experiments that were repeated a total of three times with similar results. *$P<0.05$ *vs* the corresponding value for Mock cells (Student's two-tailed *t*-test). NS, not significant.